Journal of Materials Chemistry C

ROYAL SOCIETY OF CHEMISTRY

REVIEW

View Article Online
View Journal | View Issue

Cite this: J. Mater. Chem. C, 2023, 11, 11776

Oxidative chemical vapor deposition for synthesis and processing of conjugated polymers: a critical review

Afshin Dianatdar and Ranjita K. Bose *

Received 8th May 2023,
Accepted 13th August 2023

DOI: 10.1039/d3tc01614e

rsc.li/materials-c

Oxidative chemical vapor deposition (oCVD) has developed progressively in the last two decades as a solvent-free (or dry) methodology for synthesis and thin film deposition of conjugated polymers. This method has offered new opportunities beyond traditional solution processing methods in the research of these materials. It is crucial to have a clear understanding of the differences between the solvent-free *vs.* solvent-based methodologies for synthesis and thin film deposition of conjugated polymers. Herein, the strengths and limitations of each procedure are compared in order to provide guidelines for future research and development. This review systematically approaches this comparison by first characterizing the thin films in terms of their chemical and physical properties. Then, the interfacial properties of a conjugated polymer thin film with the underlying substrate are critically compared when two different processing methods are exploited. Finally, the effect of the substrate on the coating properties and performance is reviewed.

1. Introduction

Polymers have long been considered as insulating materials, and it was only about 35 years ago that numerous reports of polymers showing conductivity emerged in the literature.[1] This was a breakthrough as until then, scientists had been dependent on inorganic materials such as metals and metal oxides for conductive properties. Therefore, the concept of a material with the flexibility of traditional polymers and conductivity of metals opened a wide scope of interest in academia and later in industry as well. The term "synthetic metals" was coined to describe these new materials, which are not metals but possess free electrons to conduct electricity.[2,3]

Department of Chemical Engineering, Engineering and Technology Institute Groningen (ENTEG), University of Groningen, 9747AG Groningen, The Netherlands. E-mail: r.k.bose@rug.nl; Tel: +31 50 3634486

Afshin Dianatdar

Afshin Dianatdar attended University of Groningen (The Netherlands) in 2017 to follow his PhD degree of chemical engineering. His research interests have been conjugated polymers, chemical vapor deposition, and their application in electrochemical energy storage devices. Upon graduation in 2022, he joined Johnson & Johnson (Belgium) as Formulation Scientist and currently involved in innovation projects around antifouling coatings for marine applications.

Ranjita K. Bose

Ranjita K. Bose obtained a bachelors in chemical engineering from Gujarat University (India) in 2006, followed by a PhD in chemical vapor deposition of polymers in 2011 from Drexel University (USA). From 2012 to 2017 she did postdoctoral research on self-healing polymers in the Delft University of Technology (The Netherlands). In 2017 she joined the University of Groningen (The Netherlands), where she is currently an associate professor of polymer engineering. She leads a team of 7 PhD students, 1 postdoctoral researcher and 3 MSc students working on chemical vapor deposition of polymer films and coatings, rheology, and structure–property relationships in polymers for self-healing applications.

The general term of "conductive polymers" encompasses a broad area of ion-conducting and electron-conducting polymers based on their mode of charge propagation.[4] For ionic conductivity, conductive polymers should be able to be easily oxidized and reduced, subsequently allowing the counter ions to move freely in the polymer matrix. This ion is either an anion or a cation. Anion movement is possible in the case of oxidized conductive polymers, resulting in a polycationic backbone, where small counter ions such as Cl^- could move along due to an anionic potential. On the other hand, when conductive polymers are reduced, cationic conductivity becomes possible in the resulting polyanionic structure.[5] However, the current review focuses only on electron conducting polymers. These polymers are also called redox polymers. Redox polymers could again be classified into different groups based on the following (see Fig. 1(a)–(d)):[6]

(a) Location of redox-active sites: (i) polymers that embed the redox-active site(s) along their backbone; and (ii) polymers that bear the redox-active site(s) in their side chains.

(b) The chemical structure of their backbone: (i) conjugated and (ii) non-conjugated.

(c) Nature of the redox center: (i) organic and (ii) inorganic.

Clearly, polymers as a result of hybrid forms of the above have also been developed during the last few decades in the attempt for new materials development with modified properties.[7] Additionally, complications resulting from the fact that the redox-active site(s) is associated with the polymer either through covalent bond(s) or *via* supramolecular interactions should also be considered for a precise distinction.[8] The following discussion only includes organic materials, in which redox groups are covalently bonded within the polymer architecture.

a. Types of electroactive polymers

i. Polymers with side chain redox sites. Insulating polymers could become electronically active *via* side-chain modification. They possess localized redox sites in their side chain, as shown in structures (1) and (2) (Fig. 2). One main advantage of these polymers is the possibility to process them using wet chemistry, circumventing a major challenge of polymers with redox groups along their backbone as would be explained later (especially the conjugated ones).[10] However, the limitation with these polymers is that charge centers are localized, limiting their mobility to only hopping between these localized redox centers.[11,12] Nevertheless, these polymers are a major category of the field and have found applications in optoelectronics, energy harvesting and storage, medicine, *etc.*[7,10,13,14]

1.1.1. Polymers with redox groups along their backbone

Non-conjugated backbone. The polymers which embed the electroactive group along their backbone, although their backbone does not have a regular alternating single and double bond, entirely fall within this group. Examples are structures (4) and (5) in Fig. 2.

Conjugated polymers (CPs). Redox-active polymers with conjugated backbones are the polymers giving fame to the field of electrically active macromolecules. In their simple definition, CPs (also called intrinsically conductive polymers) are macromolecules that have a conjugated sequence of single and double carbon bonds along their chains.[15] The history began in 1976, when Alan MacDiarmid, Hideki Shirakawa and Alan J. Heeger together reported that the conductivity of 'trans polyacetylene' could be enhanced up to seven orders of magnitude upon exposure to halogens.[16] This breakthrough opened a new era in the physics and chemistry of polymeric materials, and won them the Nobel Prize for Chemistry in 2000.[17] Polyacetylene itself was not a stable polymer and never found practical applications.[18] It stimulated the research into polymers with similar properties, which resulted in introduction of a wide range of conjugated polymers, some of the most important of which are presented in Fig. 3.

From a comparison point of view, these polymers show a range of conductivities from insulator to metallic, with most reported conductivity in the range of 10^{-5}–10^{3} S cm^{-1}, mostly lying in the semiconductive range (Fig. 4).[19] Additionally, they could combine the conductivity of a metal with flexibility of a

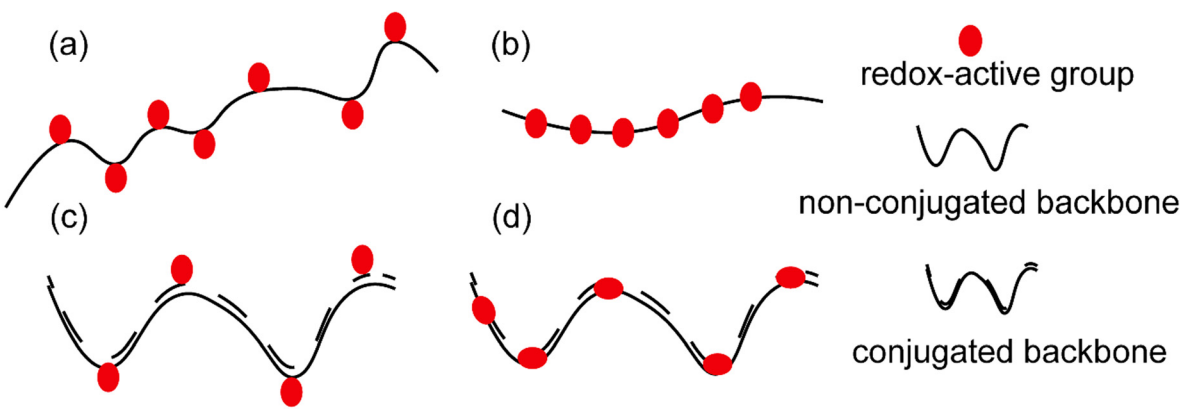

Fig. 1 A schematic representation of (a) a polymer with non-conjugated backbone bearing redox active groups (red balls) in its side chains; (b) a polymer with non-conjugated backbone containing the redox active sites along its backbone; (c) a polymer with conjugated backbone bearing redox sites in its side chains; (d) a polymer with conjugated backbone including its redox groups along its backbone.

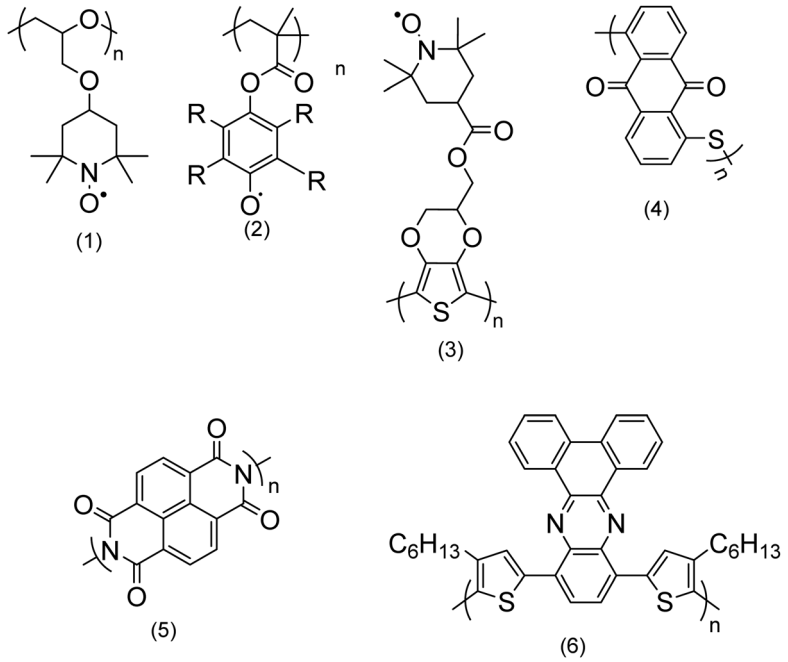

Fig. 2 Chemical structures of a few redox polymers: structures (1) and (2) are examples of non-conjugated polymers with redox sites in their side chains; structure (3) shows an example of a conjugated polymer which bears redox active sites in its side chain; structures (4) and (5) are examples of non-conjugated polymers with redox centers along their backbone; and structure (6) is an example of a conjugated polymer with redox sites along its backbone.[9]

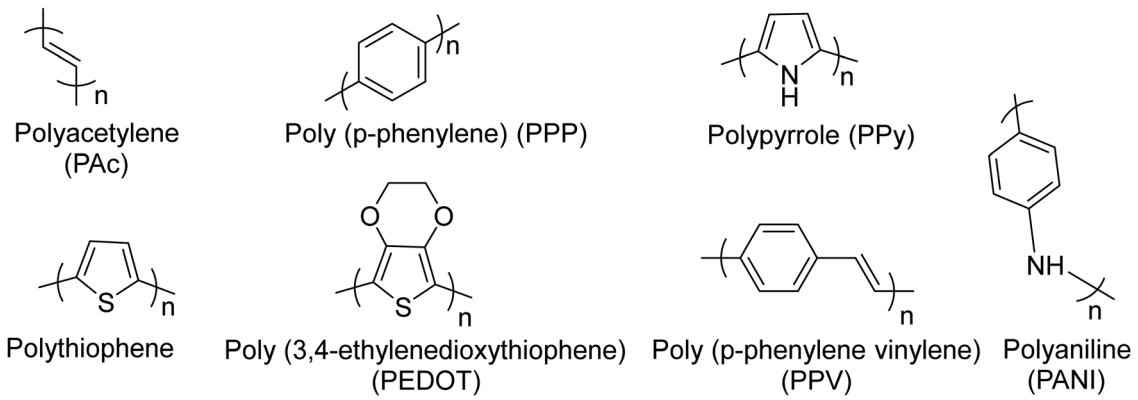

Fig. 3 Chemical structures of the most common conjugated polymers, which have been exploited readily or as the building block for the synthesis of more sophisticated redox active polymers.

polymer (in a rough sense). These all gave rise to a large body of research from the 1980s up to now.

The conjugated structures in Fig. 3 consist of adjacent carbon atoms associated together with σ-bonds that hold the structure together and orthogonal π-bonds that are delocalized and allow electron mobility within the polymer chains (intra-molecular charge transfer).[20] Additionally, inter-chain electron hopping is another factor determining the overall conductivity of a CP. From a physical point of view, materials could be divided into three categories according to the electron orbital structure, namely insulators, semiconductors, and conductors (Fig. 5).[19,21]

The determining criterion is the energy gap between the highest occupied molecular orbital (HOMO) and the lowest unoccupied molecular orbital (LUMO). For a material to show conductivity, it is required that electrons to be transferred from the HOMO (also called the valence band) to the LUMO (also called the conduction band). If such a transfer occurs, the electrons might potentially be able to freely transport within the material. The energy difference between these two "states" is called the band gap.[23] In conductors (*e.g.*, copper or gold), this gap does not exist. That is why electrons could freely move between the bands and the material. For insulators such as wood or rubber, the required energy for the transfer of an

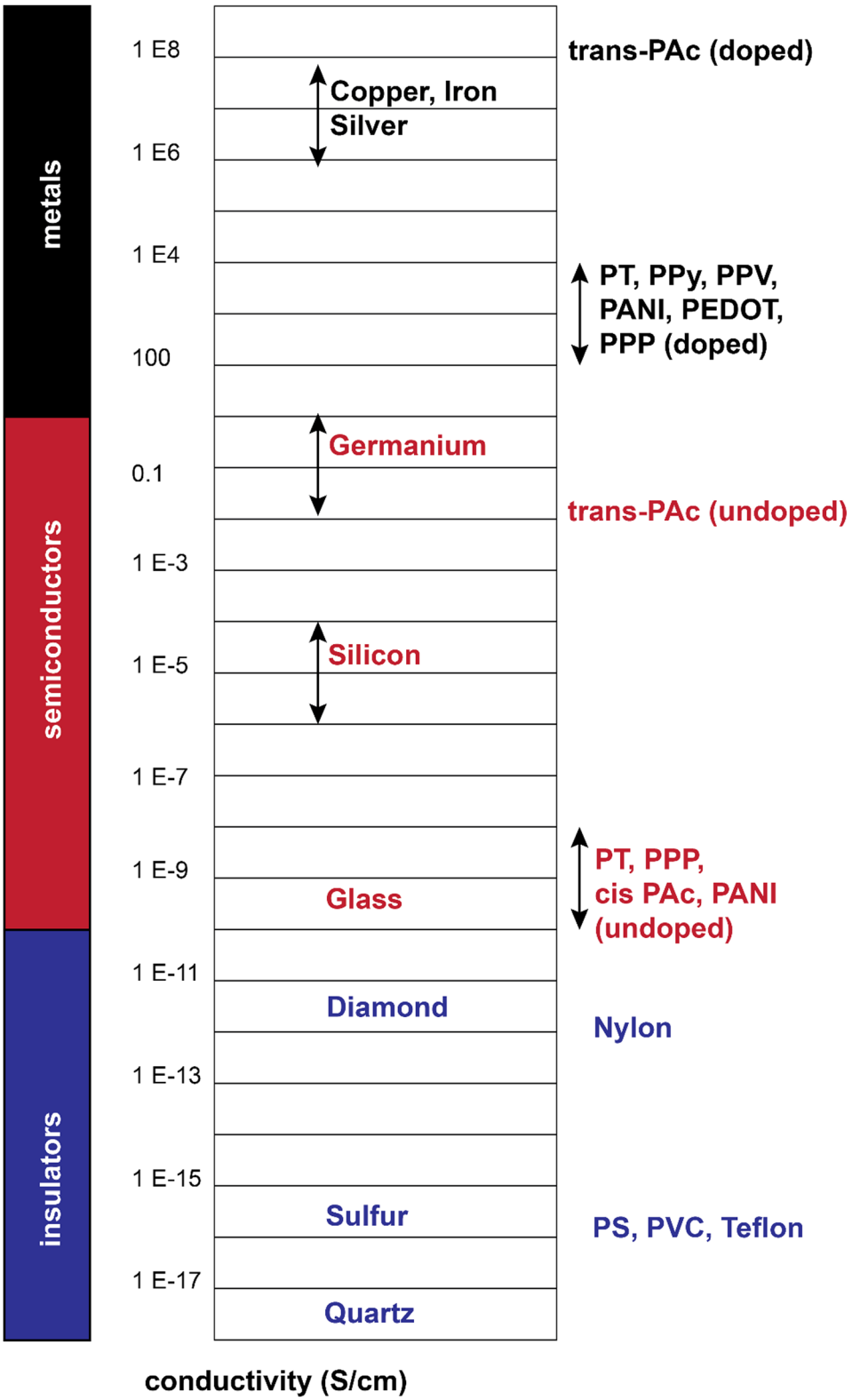

Fig. 4 Electrical conductivity of doped/undoped conjugated polymers relative to selective inorganic materials.[22–24]

electron from the valence band to the conduction band is so large (>10 eV) that makes the process very difficult or impossible.[25] For semiconductors, a certain amount of energy is required for an electron to be transferred between "valence band" and "conduction band" and for the sake of "neutral" conjugated polymers, this energy is between 3–6 eV which

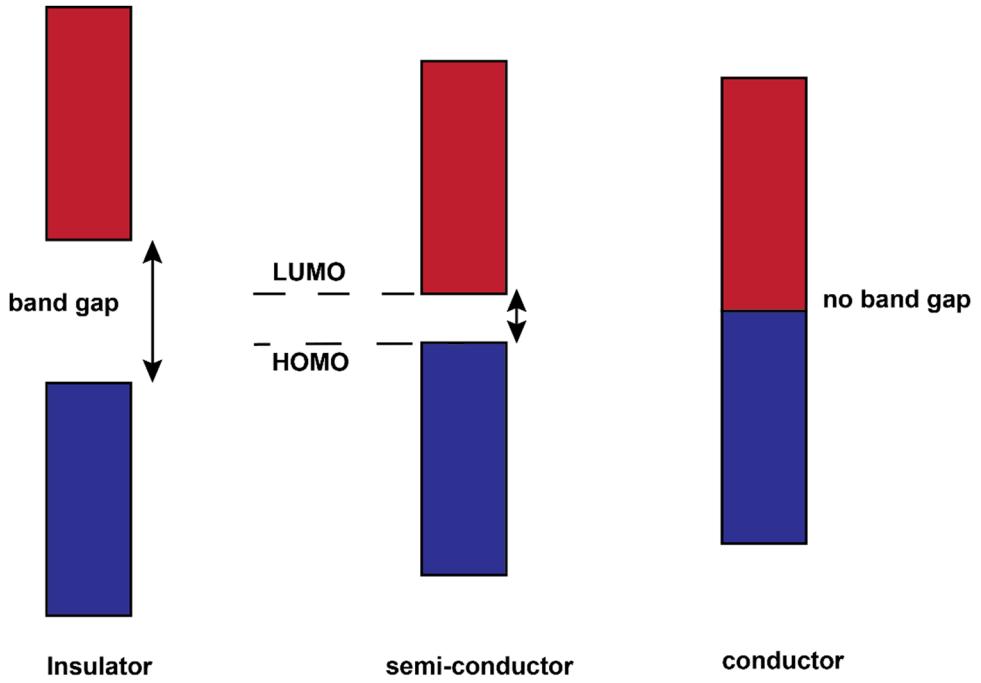

Fig. 5 Band gap structures for insulators, semiconductors, and conductors.

reduces to 1–4 eV upon doping.[19] The synthesis and processing of CPs is the main scope of the current review.

b. Synthesis (polymerization)

There are different methodologies for the synthesis of CPs including solvent-based methods of chemical polymerization, electrochemical polymerization, emulsion polymerization, and photo-induced polymerization. Selected chemical polymerization routes could also be progressed in solvent-free mode of vapor-phase polymerization, oxidative chemical vapor deposition, and plasma polymerization.[9,26–30]

The above categorization based on solvent-use is particularly relevant as CPs in their unmodified form are not soluble in common organic solvents and this complicates their initial polymerization and their further processing with the aid of solvents.[31] This should be understood within the context of common CP applications in the devices (mentioned above), in which they are often in the form of a thin film of a few nanometers to a few micrometers.[32] In other words, when CPs are synthesized (in bulk), they need to be further processed into a thin film by different coating methods such as spin coating or casting, which gives rise to challenges if the initial polymer is not soluble.[33] On the other hand, vapor-phase deposition exploits a gas-phase reactor to polymerize a thin film of CPs on a surface from reactant vapors. Although the vapor-phase synthesis of PPy dates back to 1986,[34] a systematic protocol was pioneered by K.K. Gleason[35] of MIT in 2006. In this method, which is basically equal to oxidation polymerization without use of solvent, the monomer and the oxidant are separately metered into a vacuum chamber in the initial step and react directly onto the surface of a substrate resulting in a thin film.

c. Properties and applications

As mentioned above, CPs combine the conductivity of a metal with the flexibility of a polymer. This gave rise to a large body of research from 1980s up to now for a wide range of applications including but not limited to organic electronics: organic photovoltaics, field-effect transistors, light-emitting diodes; energy storage devices: batteries, supercapacitors, fuel cells;[36–40] medical devices and procedures: sensor, drug delivery, tissue engineering, actuator;[41–44] and other fields like corrosion,[45–47] textiles,[48] gas/liquid separation,[49,50] and catalysts.[51]

Electrical conductivity in CPs is a combination of electron and ion mobility. The ionic conductivity of CPs is poorly understood due to the lack of comprehensive studies.[52] For ionic conductivity in solid-state polymers, the polymeric host should act as a solvent for the ions.[53] However, being solids, they are inherently poor solvents, and therefore, their ionic conductivity only finds relevance in certain applications where liquid-based solvents are also present such as electrochemical energy storage devices. In this regard, although a common resistivity measurement method *via* a four-probe technique does not distinguish between ionic and electronic conductivity of a solid CP,[54] it is reasonable to think that the dominant mechanism of charge transfer in these materials stems from electrical conductivity.

d. Aim and scope

As could be expected, each of the above methods offers their own advantages over the other, which makes either of them

preferred under certain circumstances. Considering the importance of CPs in fundamental and applied research as well as potential industrial applications, there are numerous review papers, books (chapters) on CPs and their properties,[55–60] an overview of different synthesis routes[61,62] such as catalytic polymerization,[33] electropolymerization[63,64] or vapor-phase polymerization,[65–68] along with their applications in different fields such as electrochemical energy storage devices or medical sensors.[69] For the case of vapor-phase polymerization and oxidative chemical vapor deposition, previous reviews periodically detailed and updated the procedure of conjugated polymer synthesis, materials chemistry, the reaction mechanism, the properties of the polymers synthesized, and the structure–property relationships. These reviews significantly contributed to advancing the state-of-the-art. However, there is no systematic review outlining how oCVD (or other vapor-phase synthesis techniques) compares to the other solvent-based in different aspects of CP thin films including synthesis routes, polymer properties and processing aspects. The clarity in this case is of utmost importance as the synthesis method not only determines the possibility of using different synthesis routes but also vastly affects the properties of the final polymer.

The remainder of this review critically addresses how these methods differ. First, a brief overview of each of the polymerization routes listed above is provided. Then, the most developed methodology in each category *i.e.*, chemical synthesis (as a solvent-based method) and oxidative chemical vapor deposition (as a solvent-free method) is chosen for more comprehensive discussion and comparison. We will discuss in detail three sections: thin film, thin film–substrate interface, and substrate. It should be noted that each of these components is not independent of each other. The advantages and limitations of oCVD compared to solution processing are outlined following the reports in each field. It is worth mentioning that there are certain aspects of thin film deposition (on a substrate) that have not been directly addressed in oCVD research reports given that it is a relatively new field. For these aspects, a critical discussion of how oCVD may differ from solution processing is provided, analyzing the basic physics and chemistry of vapor-phase *vs.* solution-phase processing of polymers from the literature.

2. Solvent-based methods

a. Chemical polymerization

Chemical polymerization is the most developed technique for polymerization of conjugated polymers. It also serves as a platform for most of the other methods. Chemical polymerization broadly includes oxidation polymerization and organometallic polycondensation. In the former method, an oxidant is used to form a radical cation of the monomer. Then, two such cations form a C–C bond, resulting in a radical dication. This coupling continues till the formation of a conjugated polymer. An example for oxidation polymerization of polypyrrole is provided in Scheme 1.[70,71]

Organometallic polycondensation proceeds where a bis-halogenated monomer undergoes C–C bonding *via* different coupling methods including Kumada, Suzuki–Miyaura, Stille, and Negishi polycondensation mechanisms.[33,72,73] Scheme 2 provides the general route of these reactions, details of which are beyond the scope of the current review and could be followed in the cited documents. For simplicity, from now on, we will use organometallic polycondensation as an umbrella term for all these methods.

b. Other synthesis routes

Electrochemical polymerization is another popular method for the synthesis of CPs. It uses an electrochemical cell consisting of a working electrode, a counter electrode, and a reference electrode dipped into a flask containing the monomer-dissolved in a solvent. The mechanism is similar to the oxidation polymerization explained above, albeit the oxidation is provided by the electrical current rather than an oxidant. In this method, a thin film of polymer is directly synthesized and formed on the surface of the working electrode, which has to be a conductive surface.[74]

The next step is emulsion polymerization, wherein an organic monomer is first dispersed in an aqueous medium with the aid of a surfactant. An oxidant is then added to the solution, triggering the oxidation polymerization and resulting in (nano)particles of the CP dispersion.[75]

Finally, photo-induced polymerization is a comparatively newer method. Photons are used to initiate and proceed polymerization of a number of CPs. It is categorized into three different mechanistic pathways:[28] (i) Oxidative radical polymerization, which was pioneered by Shimidzu *et al.*, has been used for a range of electron-rich monomers such as thiophene. In this method, a solution containing a monomer, an electron acceptor (such as CCl_4), and a salt (*e.g.* omnium salt) is irradiated with photons (of a certain wavelength), which triggers electron transfer from the monomer to the electron acceptor. This is followed by monomer–monomer coupling, deprotonation, and so forth to result in CP thin films.[76–78] (ii) Cationic oxidative polymerization has been reported as a solvent-free polymerization method for a thienothiophene derivative. As the authors proposed, the C–Br bond of the bromine-modified thiophene derivative is broken as a result of photolysis. This releases elemental Br_2 which initiates the polymerization by monomer addition to the cationic chain and elimination of HBr.[80] (iii) Reductive polymerization that has been exploited for the polymerization of electron-deficient monomers such as benzotriazole and thienopyrazine. The synthesis mechanism was believed to proceed *via* chain growth-free radical polymerization. It was a solvent-based reaction using LiCl as a reductant and the reaction was initiated with light having a wavelength in the range of 400–626 nm.[81]

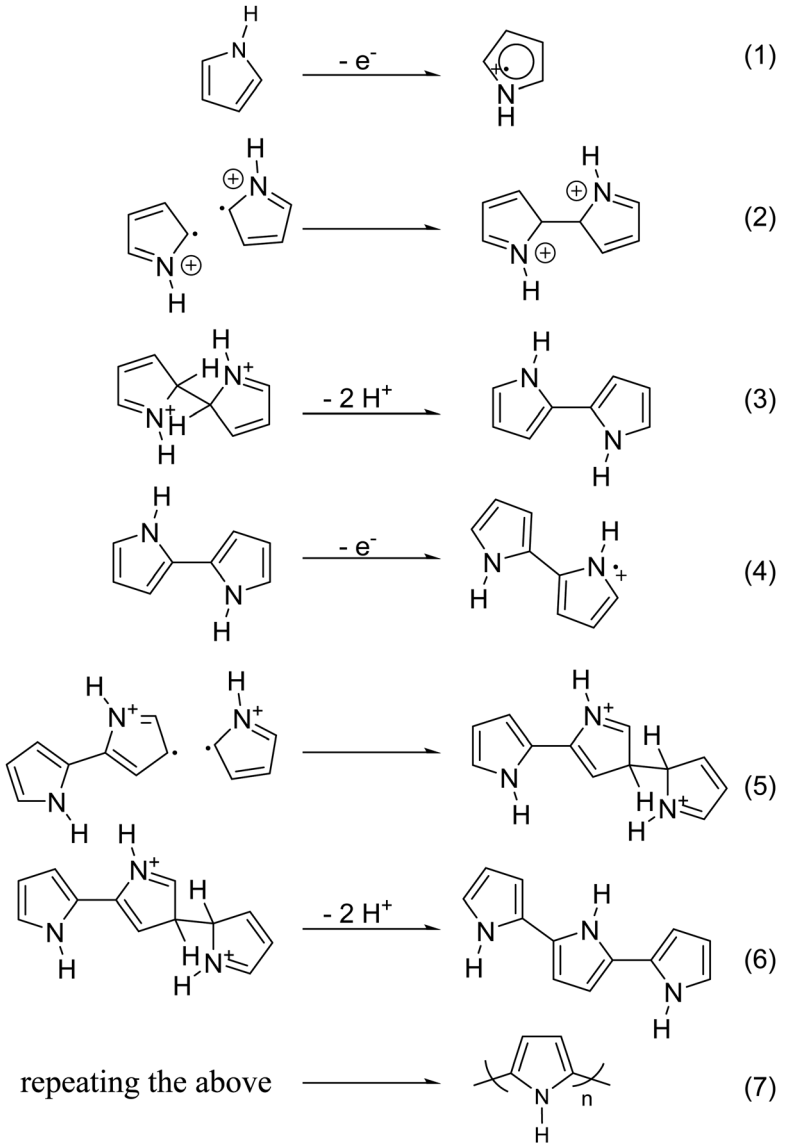

Scheme 1 Oxidation polymerization of PPy, based on the reaction mechanism proposed by Diaz *et al.*[79]

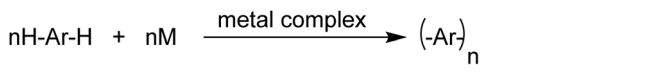

H: Halogen
M: Metal or reducing agent (such as Mg, Ni(0) (complex), Zn)

Scheme 2 The general scheme for organometallic polycondensation for polymerization of CPs.[33]

3. Solvent-free method: oxidative chemical vapor deposition (oCVD)

The general mechanism of all solvent-free methods is based on an initial oxidation of reactive monomers: the same as oxidation polymerization in the solution phase. For a long time, a common practice was to first oxidize the substrate (to be coated) with an oxidizing agent and then to expose the pre-treated substrate to vapors of monomers. In this way, the monomers should be first adsorbed on the surface of the substrate under reduced pressure and then activated by interactions with the oxidant present on the surface of the substrate. The method was named vapor-phase polymerization (VPP). It may be noted that although this method is frequently referred to as a solvent-free method in the literature, a solution of the oxidant is used for pre-treating the substrate.[82] Another solvent-free method is plasma polymerization, which is expected to proceed similarly to oxidation polymerization. The difference is that instead of an oxidant, plasma is used for the initial activation of the monomer and subsequent cross-couplings where chemical structure and stoichiometry are not reliably controlled.[83–94]

Finally, in the most developed solvent-free methodology, both the oxidant and the monomer are vaporized and metered into a gas-phase reactor under reduced pressure. They are then adsorbed on the surface of a substrate and initiate

polymerization and film formation at the same time.[35] This method was named oxidative chemical vapor deposition (oCVD) and is the subject of the current review.

Reactor design for oCVD

The early design for the oCVD reactor was inspired by the preceding works in the field of vapor phase material syntheses such as initiated chemical vapor deposition, metal–organic chemical vapor deposition, plasma-enhanced chemical vapor deposition, and atomic layer deposition.[95–98] Building upon them as well as based on one pioneering work reported by Mohammadi *et al.*,[34] a modified version of the oCVD reactor was developed in the group of K.K. Gleason at MIT and reported in 2006.[35] The reactor consisted of a vacuum chamber with a stage at the bottom, the temperature of which could be controlled by water coolant. A crucible was placed under the chamber for vaporizing $FeCl_3$, which could then be introduced into the reactor with argon (acting as a diluent) in the vertical direction and parallel to the EDOT flow. The monomer and the oxidant would be adsorbed on the reactor surface and oxidative polymerization would commence (Fig. 6(a)). Shortly after this primary design, the reactor configuration was changed by inversing the stage position under the ceiling and crucible at the bottom, in order to avoid substrate contamination with $FeCl_3$ particulates.[99] Also, the EDOT monomer flow was introduced into the chamber at a 90° angle relative to the oxidant flow direction (Fig. 6(b)). This reactor configuration is still in use up to today. However, other research groups again came up with reactor modifications. For example, the group of K.K. Lau changed the oxidant from $FeCl_3$ (a solid) to $SbCl_5$ (a liquid) and placed the substrate back at the bottom of the chamber (Fig. 6(c)) for deposition of polyaniline or polythiophene.[100,101] An alternative reactor configuration exploited two crucibles inside the chamber allowing the vaporization of relatively high M_w monomer in addition to the oxidant crucible (Fig. 6(d)).[102] However, this configuration used a smaller surface area of the substrate compared to the original one (26–52 cm^2).[30] Finally, in a more recent configuration and with inspiration from molecular layer deposition reactors, Andrew *et al.* adopted a hot-wall tubular shape reactor, in which the monomer and the oxidant would flow in the opposite direction and in parallel to the long-axis tubular direction (Fig. 6(e)).[103] In this way, the monomer and oxidant mix in a controlled manner during their residence time above the substrate. This configuration has been used for both solid and liquid phase precursors, giving flexibility in reaction design.

4. CP thin films

The first (and in a sense the most) important aspect of a thin CP film on a substrate is the properties of the film itself. Using the electronic property as the evaluation index, there are mainly five critical aspects that contribute to the thin film performance, namely (i) chemical structure, (ii) conjugation length, (iii) crystallinity, (iv) packing, and (v) doping. These aspects are not mutually exclusive as mentioned before. Below, each factor is discussed in more detail.

a. Chemical structure

The nature of a CP itself primarily determines the electronic properties of the thin film. For example, polythiophenes and their derivatives usually show higher conductivities than polyaniline.[104,105] Therefore, the first aspect to consider is to compare the range of monomers that can be polymerized by each method. Table 1 provides an overview of the monomers polymerized by oCVD reported until now along with the reported values (if applicable) of their electrical conductivities. In principle, oCVD replicates oxidation polymerization and should therefore be applicable to the various conjugated monomers polymerized by oxidative polymerization. It was also possible to polymerize 3-thiopheneethanol, a direct polymerization of which does not proceed either chemically or electrochemically.

There is a need for an initial modification step to protect its hydroxyl group to avoid its nucleophilic attack in a polymerization environment. Although with oCVD, it was possible to directly copolymerize it with EDOT in a one-step oCVD without the need for protection of hydroxyl groups.[107] Yet, important CPs like poly(*p*-phenylene) (PPP) or poly phenylene vinylene (PPV) are excluded from oxidative polymerization (therefore oCVD as well). However, it is worth mentioning that for the case of PPV, alternative CVD routes taking advantage of precursor pyrolysis have been done before, which could be a basis for other non-catalytic routes for the synthesis of CPs.[108–111]

With chemical methods and in particular with organometallic polycondensation, a wide range of monomers can be synthesized that is beyond the scope of oCVD. An immediate reason for this is the use of catalysts (in their solid form) which is not possible to implement in the current state-of-the-art vapor-based oCVD method. Another aspect is that organometallic polycondensation often involves multi-step reactions, while oCVD is a one-step process. Therefore, oCVD is not able to provide comparable control over the structure of CPs as it is a one-step, non-catalytic method.[112,113]

In addition to the different properties resulting from CPs synthesized *via* different polymerization methods, oxidation polymerization is more limited in terms of the variety of monomers that are possible to polymerize as compared to organometallic polycondensation.

One primary consideration of oCVD is the vapor pressure of monomers under deposition conditions. A monomer should have sufficiently high vapor pressure under the deposition temperature and pressure to be introduced into the reactor in the gas phase. This often becomes challenging as the monomer gets bulkier, which is associated with higher M_w, melting point, and boiling point. These non-volatile monomers tend to rapidly lose their kinetic energy upon entrance into the CVD chamber and condense, which restricts their further interaction with oxidants and polymerization.[103] Despite this general challenge, the case for the deposition of porphyrin derivatives (with $M_w >$ 400 g mol^{-1}, melting point >350 °C) proved that with an

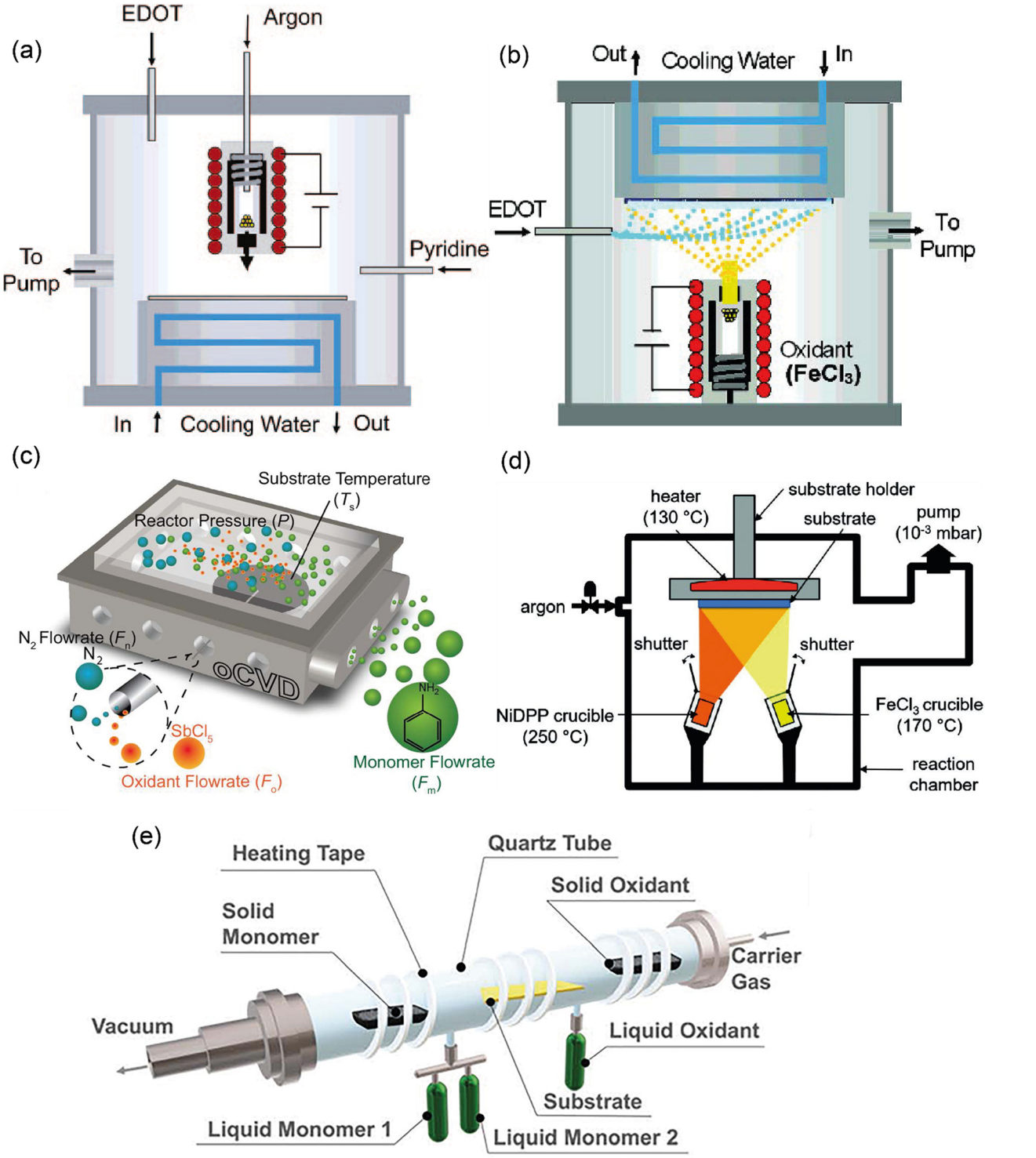

Fig. 6 Different reactor configurations with (a) stage on the ceiling, with oxidant vaporizing by crucible at the bottom, and oxidant and monomer flow with 0° relatively. Reprinted with permission from.[35] Copyright (2006) American Chemical Society. (b) Stage on the bottom, with oxidant vaporizing by crucible on the ceiling, and oxidant to monomer flow with 90°. Reprinted with permission from.[99] Copyright (2007) American Chemical Society. (c) Stage on the bottom, with liquid oxidant and monomer flowing into the reactor at 90°;[101] (d) with a substrate on the ceiling, and solid/oxidant vaporizing by crucible flowing at an angle <90°;[106] (e) tubular reactor configuration with monomer/oxidant (solid/liquid) flowing into the reactor at 180°. Reproduced from ref. 30 with permission from The Royal Society of Chemistry.

accurate experimental design and the deposition conditions, it was possible to expand oCVD to heavier monomers.[106] Cardenas-Morcoso *et al.* took porphyrin-based CP research to the next level by synthesizing a wide range of 5,15-diphenyl

Table 1 Library of the monomer/oxidant combinations used for the synthesis of conjugated polymers using oCVD

Monomer	Oxidant used	Conductivity (S cm^{-1})	Ref.
 Thiophene	$FeCl_3$, $VOCl_3$, $SbCl_5$	2.7×10^{-5}–70	125–128
 Pyrrole	$FeCl_3$, $SbCl_5$	2–180	21,129,130
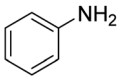 Aniline	$SbCl_5$	NA	101
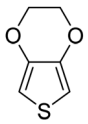 EDOT	$FeCl_3$, Br_2, $CuCl_2$, $SbCl_5$, $VOCl_3$	9.1×10^{-4}–6259	99,131–140
 Selenophene	$FeCl_3$	2–35	141,142
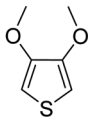 3,4-Dimethoxythiophene	$FeCl_3$	10	143
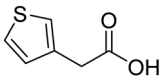 3-Thiophene acetic acid	$FeCl_3$, Br_2	10^{-4}–10	129,144,145
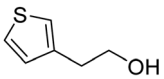 3-Thiophene ethanol	$FeCl_3$	Non-conductive	107,146
 1,3-Dihydroisothianaphthene	$FeCl_3$	10^{-3}–1	147
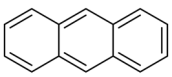 Anthracene	$FeCl_3$	NA	148
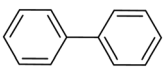 Biphenyl	$FeCl_3$	NA	148
 3,4-Dimethyl thiophene	$FeCl_3$	NA	103,149
 3-Methyl thiophene	$FeCl_3$	NA	103,149

Table 1 (*continued*)

Monomer	Oxidant used	Conductivity (S cm^{-1})	Ref.
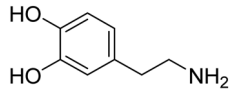 Dopamine	H_2SO_4/Na_2SO_4	0.4	150,151
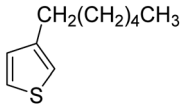 3-hexylthiophene	$FeCl_3$	4×10^{-4}–4	152
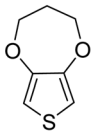 3,4-Propylene dioxythiophene	$FeCl_3$	106	103,149
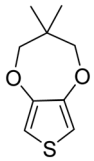 3,4-(2,2-Dimethylpropylenedioxy) thiophene	$FeCl_3$	31	103,149
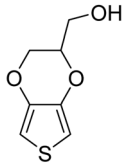 Thieno[3,4-b]-1,4-dioxin-2-methanol	$FeCl_3$	1.6	103,149
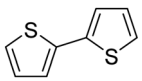 2,2′-Bithiophene	$FeCl_3$	NA	103,149
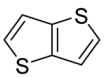 Thieno[3,2-b]thiophene	$FeCl_3$	NA	103,149
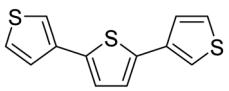 3,2′:5′,3″-Terthiophene	$FeCl_3$	NA	103,149
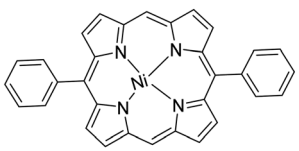 Nickel(II) 5,15-diphenyl porphyrin	$FeCl_3$, $CuCl_2$, $(Cu(ClO_4)_2 \cdot 6H_2O)$. $FeCl_3$	3.6×10^{-2}	102,106
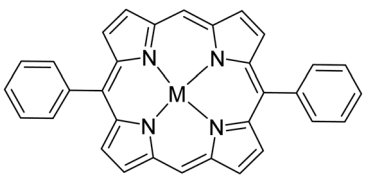 M = MDPP; M = Co, Cu, Mg, Zn, Pd, Pt, Ag, Ru, Ag, and FeCl) 5,15-diphenyl metalloporphyrins	$FeCl_3$	NA	114

metalloporphyrins (MDPP; M = Co, Cu, Mg, Zn, Pd, Pt, Ag, Ru, Ag, and FeCl; see Table 1).[114] This was particularly appealing due to the MDPP application for solar-based energy generation devices, but difficulty in its processing. Another strategy could be using a nitrogen bubbler to facilitate monomer vaporization and flow into the CVD reactor.[115] One concern still remains that even with successful deposition of such monomers, the deposition rate could be possibly very low, the same bottleneck that atomic layer deposition faces.[116]

On the other hand, chemical synthesis and solution polymerization depend on the persistent solubility of the reactants as well as the growing polymeric chains in the reaction medium (solvent). However, alternating single and double bonds in conjugated chains of CPs are highly rigid, causing the chains to aggregate in the solvent rather than being dissolved. As a result, with the addition of each monomeric unit to a growing chain in a reaction medium, the tendency of the chain to precipitate out of the solvent becomes higher.[117] This puts a limit on how large the chains could propagate before precipitation. As a solution to this challenge, conjugated monomers are modified with alkyl groups at the 3rd and/or 4th position. Such a limitation however is not applicable to oCVD, simply because it is a solvent-free method. Therefore, oCVD offers the possibility for direct synthesis of common conjugated monomers. This specific solvation issue becomes more relevant in processing and the final film properties are discussed further in the following sections.

p-type *vs.* n-type CPs. When it comes to CPs, an important classification directly linked to their potential applications and properties is either they are a p-type or an n-type CP, mimicking the terminology of inorganic semiconductors.[118] However, here, a clarification should be made between ''p-type or n-type doping of CPs'' *versus* ''p-type or n-type CPs''.

In principle, a conjugated polymer could be oxidized or reduced by a dopant. As a result, the polymer turns into a polycation or polyanion, whose charges would be compensated by the counter ions from the dopant. The former is called p-type doping while the latter is called n-type doping of CPs. With this consideration, it could be hypothesized that any CP can be potentially p-doped or n-doped if strong enough oxidizing or reducing agents are used and/or by application of electrochemical methods. However, in practice, the most common CPs are more prone to oxidation. Their reduction, while studied theoretically and shown also in practice for a few of them, is challenging and might need very strong reducing agents like alkali metals *e.g.*, sodium naphthanilide, sodium/potassium alloys, and lithium iodide.[19,119,120] The main reason for this challenge lies in the electron-rich conjugated backbone of CPs in general. Nevertheless, due to the desired properties that electron-conducting CPs could offer, there has been enormous research on the modification of conjugated monomers to alter their orbital structure and make their backbone electron deficient, easing the process of n-doping. In this context, the CP_S which readily tend to be oxidized rather than reduced have been frequently termed as p-type CPs, while the other modified CPs with electron gaining tendency have been called n-type CPs.[121–124]

Returning to the discussion on comparing the synthesis routes of CPs, as polymerization of n-type CPs often involves catalysts, it has been excluded from oCVD practice.[121,153–155] Recently, Woods *et al.*[156] reported a catalyst-free protocol for the synthesis of n-type CPs, although their precursors (*e.g.* lithium salt) are beyond the current scope of polymer CVD in general due to its extremely low vapor pressure at room temperature. Generally speaking, the electron-rich structure of common CPs (Fig. 3) needs to be modified with an electron withdrawing group in order to be able to accommodate an excess electron upon reduction. However, in oCVD, these-electron-rich structure is exactly the reason for the sp^2–sp^2 carbon coupling, making the process challenging. Nevertheless, Bilger *et al.*[157] attempted to polymerize a thiophene–cyclopentadienone–thiophene triad in which the thiophenes were electronically decoupled from cyclopentadienone and were able to engage in C–C couplings upon exposure to another monomer in the presence of $FeCl_3$ gas. This attempt of course opens new directions in the field of oCVD. However, there are some concerns that should be considered about this protocol in parallel. First, although ultraviolet photoelectron spectroscopy results suggested a low-lying valence band level (which is essential for n-type behavior in CPs), a donor–acceptor–donor (D–A–D) structure has not been considered among the best strategies for n-type monomer design (common strategies donor–acceptor (D–A) with strong A, D–A with weak D, A–D–A and A–A[121]). Second, if the donor has to be electronically decoupled from the acceptor in order to preserve its ability for C–C bonding, the acceptor can no longer apply its electron-withdrawing effect on the donor in order to provide the backbone with space for electron injection. Therefore, more investigation into this strategy is necessary to understand its potential.

b. Conjugation length

A charge carrier has a limited path to travel along the chain of a CP. Such a path is called the (effective) conjugation length, which is affected by M_w and the microstructure of the CP.[158] When it comes to electron mobility along a polymeric chain as well as intermolecular charge transfer, with a more extended chain there is more space for the carrier to travel along the chain.[159] On the other hand, the position at which monomers link to each other also impacts the electron mobility in the chain. This is called structural regularity and it could have three configurations as discussed later. Finally, there is the conformational regularity that impacts electron transfer in a single polymeric chain. For example, a chain twist could compromise carrier mobility as well.[160,161] The combination of all these factors determines the effective conjugation length of CP polymeric chains.

M_w of a polymer determines how long the chains are and therefore directly influences the conjugation length.[162,163] In solution synthesis, the growing polymeric chains need to continuously maintain their solvation in their reaction medium as additional units are added. However, as mentioned in the previous section, the rigid backbone of CPs in their basic

chemical structure makes their solubility a challenge in the common organic solvents. Indeed, they tend to result in fine aggregates at best when so-called ''good'' solvents are used.[27,164–166] Therefore, a growing chain of CP is highly susceptible to precipitate at oligomeric length when polymerizing in solution.[167–171] To address this issue, researchers have came up with the idea to modify the monomer structure (*e.g.* adding an alkyl chain to the 3rd position) in order to enhance the solubility of the growing polymers in the reaction medium. This of course gives rise to partial distortion in the conjugation of the resultant CPs, negatively impacting their electronic properties.[160,172,173] Another parameter influencing M_w is the CP crystallinity which would be discussed in the microstructure section.

As oCVD is a solvent-free method, the above concerns about solvation of unmodified conjugated monomer are not applicable. Therefore, oCVD might have the potential to grow CPs with higher M_w. Although *via* an indirect assessment, there have been reports revealing that oCVD provides control of conjugation length, because of the difficulty in estimating M_w of CPs in general, it was not possible to test the above hypothesis on oCVD potential to grow high M_w CPs. Yet, indirect methods showed how fine-tuning deposition conditions could increase the conjugation length.

In an early report, Im *et al.*[99] observed that increasing the deposition temperature of PEDOT from 15 °C to 100 °C resulted in a continual decrease in the π–π transition energy measured by UV-vis spectroscopy. In another report, Goktas *et al.*[107] copolymerized EDOT and 3-thiophene ethanol by oCVD and observed that the monomer feed ratio impacts the number of each unit in the final polymeric chains analyzed by AP-MALDI-HRMS spectroscopy; they attributed this observation to the conjugation length in part. In another research, PITN[147] was synthesized by oCVD and it was observed that by increasing the deposition temperature from 70 °C to 130 °C, the band gap decreased from 1.14 eV to 1.05 eV. Additionally, the Raman and FTIR peaks downshifted continuously with increasing deposition temperature. These all were attributed to a higher conjugation length. Cheng *et al.*[103] observed a higher oxidation potential (deeper HOMO) with reduced conjugation length. Smolin *et al.*[174] synthesized PANI with oCVD and attributed the peak of 825 cm^{-1} to higher M_w PANI. However, in this case, it was observed that 1590 cm^{-1} and 1580 cm^{-1} peaks of quinonoid and benzenoid of aniline polymer shift to 1580 cm^{-1} and 1505 cm^{-1} for aniline oligomer.[175]

Borrelli *et al.*[126] analyzed oCVD-grown unsubstituted PTs using Raman spectroscopy. As had been suggested before, the C=C antisymmetric stretching vibration would lose intensity and downshift upon a higher conjugation length. Using this as the index, the research showed that the PT film deposited at 1 mTorr resulted in the shortest conjugation length. However, the other deposition pressures (75, 150, and 300 mTorr) all showed somewhat similar Raman (as well as UV-vis) spectra to each other. This suggests that pressure could be used to modulate the conjugation length to some degree.

Another parameter is the type of oxidant. Deposition of PEDOT with two different oxidants Br_2 and $FeCl_3$ revealed that bromine was able to result in a higher conjugation length, which was inferred from spectroscopy. This was attributed to a higher oxidizing strength of bromine compared to iron chloride.[176]

When it comes to structural regularity, organometallic polycondensation has been the method of choice for the synthesis of CPs, allowing 2,5 coupled polythiophenes.[33] There could be three types of C–C linkages, which are named as tail–tail (TT) for 5,5 C–C coupling, head–tail (HT) for 2,5 C–C coupling, and head–head (HH) for 2,2 C–C coupling (Fig. 7(e)). HT coupling represents a regularity, control of which has not been possible by oxidation polymerization. The results showed that oxidation polymerization forms random 2,4 linkages, which undermines the effective conjugation length.[177–182] Therefore, oCVD may not inherently be able to compete with chemical methods in forming regioregular CPs. However, there is an early report of the synthesis of regioregular polythiophenes with the controlled introduction of oxidants into the medium in multiple time spans, which may give a hint in oCVD processing as well.[183] The microstructure of CPs is more extensively discussed in the next section.

Regarding M_w of CPs synthesized by oCVD, one concern could be reactants ''accessing'' a polymerization spot of a growing chain, which might be undermined by the lower diffusion rate of the reactants to the potential chains embedded in the already-formed film. This phenomenon of diffusion into the polymer film is not yet understood.

c. Microstructure

As a polymeric chain has limited length, a carrier moving along the chain needs to hop between them at some point. This is called inter-molecular charge transfer. In this regard, how the polymeric chains are arranged relative to each other determines the polymer microstructure and electron mobility. This topic could be discussed in terms of crystallinity and thin film packing.

i. Crystallinity. From the morphological point of view, ordered crystalline domains within the microstructure of a CP coating favor charge carrier mobility.[187–190] The formation of ordered crystal grains for a number of CPs has been realized at two levels: either by their structural engineering and/or by tuning the processing conditions during/after film formation[191–193] An illustration of a semicrystalline P3HT consisting of crystal lamellae and amorphous chains is shown in Fig. 7(a).

From a structural perspective, M_w and the structure of the side chains can influence the tendency of the CPs for crystal nucleation and growth.[192,194] For unmodified polymers of poly(arylene)s, crystallinity seemed to be associated with a lower M_w. As established before, poly(arylene)s – and so other CPs – are modified by side chain alkylation for better solubility. An enhanced solubility also allows for obtaining a higher M_w polymer during synthesis, which resulted in a less crystalline polymer.[33] On the other hand, comparing alkyl-modified

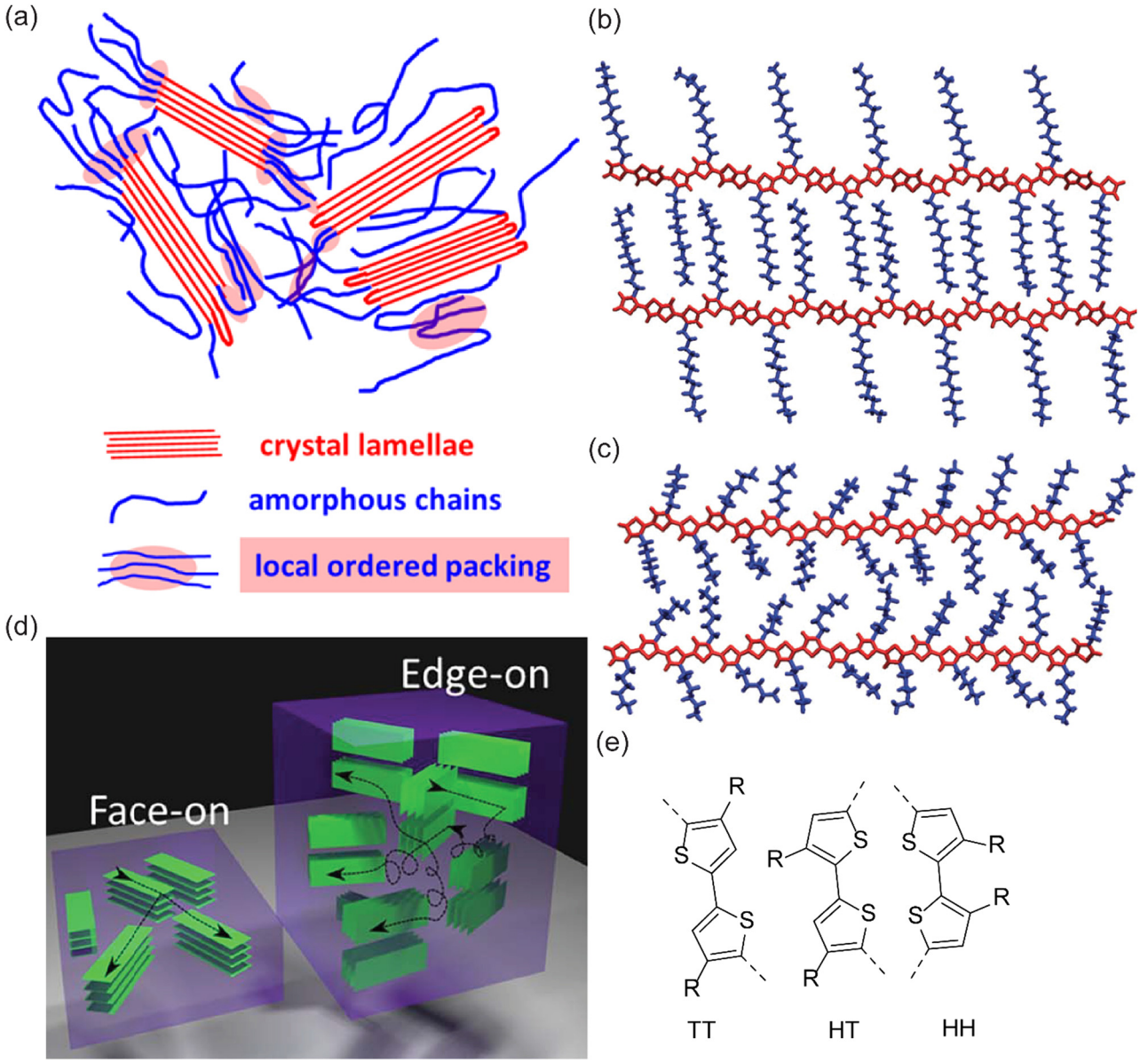

Fig. 7 (a) An illustration of P3HT morphology comprising crystalline and amorphous phases. Reprinted with permission from.[184] Copyright (2016) American Chemical Society; (b) and (c) thiophene-based CP with alkyl side chains that are interdigitated and randomly oriented, respectively. Reproduced from ref. 185 with permission from The Royal Society of Chemistry. (d) Illustration showing face-on *vs.* edge-on PEDOT orientation;[186] (e) possible C–C bonding of two thiophene groups during polymerization of poly(thiophene) namely TT, HT, and HH.

polymers within themselves, Zen *et al.* reported that the crystallinity of P3HT decreased significantly with lower M_w.[194] Yet, an additional aspect regarding M_w would be the folding behavior. Again, in the case of P3HT, when M_n surpasses a critical value of 10 kDa, the chains will transit from the extended to the folded conformation, which requires the balancing of an energy barrier to unfold and form ordered crystals.[59] Additionally, the structure of the alkyl-side chain impacts the crystallization tendency as well. If the alkyl structure is linear, resulting in a symmetrical CP structure, an improved crystallinity could be expected; while for branched side chains usually desired for better solubility, the crystallinity is undermined.[192]

After the synthesis of CPs, their solution is coated on the surface of a substrate, followed by solvent evaporation and film formation. Film morphology highly depends on the processing method and history. There are reports that the crystallinity could be controlled by the aid of solvent–polymer interaction[60,191,195,196] and film annealing after deposition.[197,198] The type of solvent and substrate surface features are the two main parameters affecting the crystallization of CPs. Sanda *et al.* used four different solvents for the processing 2,7-dioctyl[1]benzothieno[3,2-*b*][1]benzothiophene, and observed that a higher boiling point solvent resulted in larger polycrystalline domains.[199] This is attributed

to a lower evaporation rate of solvents with higher boiling points, allowing more time for crystals to grow. The same results have been noticed in other reports, suggesting a universal trend.[191,195]

Next, the substrate surface properties influence crystal nucleation and crystal growth. Physical and chemical properties of the surface including surface microstructure, roughness, and surface energy impact the interfacial interaction between substrate and solution. This controls the wetting behavior, the evaporation rate and the morphology development. In an interesting report, Zhang *et al.* showed that lowering the surface energy of the substrate by different functionalization groups, higher crystalline CP films were obtained. This was attributed to a lower penalty for heterogeneous nucleation of crystals.[193] An additional aspect is the substrate's viscoelastic properties. In a report, Kim *et al.* vapor deposited pentacene film on the surface of a number of polymeric substrates at different temperatures. They observed that in case the temperature surpasses the glass transition temperature of the substrates, nucleation density is prompted yet its growth into larger grains is disrupted. However for rigid substrates (below T_g), an increase in temperature favors the formation of larger crystal grains.[200] This could be understood in a broader context of interfacial dynamics between CPs solution and the substrate. In this regard, Diao *et al.* used a diketopyrrolopyrrole-based CP as a model compound and worked toward a general design rule for substrate-directed CP crystallization. They experimented with a template substrate modified with ionic liquids and studied how enthalpy of adsorption could be used as an index to quantify template–CP interaction. It was concluded that an increase in interaction at the interface is associated with a higher degree of crystallinity and larger domain size by the facilitation of CP nucleation *via* dynamic interaction.[201]

After solvent evaporation, an additional step of annealing has been shown to induce crystallization in certain cases.[191,197,198] In another report, Jo *et al.* showed that exposing P3HT solution to a non-solvent, the π–π interaction of P3HT chains is encouraged by the unfavorable interaction of the polymer and its non-solvent, facilitating the crystallization of P3HT nanofibers.[202]

Another strategy has been using a template, which could assist the formation of crystalline domains during thin film processing.[203] Through the so-called template-assisted crystallization, features of a surface including its roughness could stimulate crystallization by using a template, which favors the formation of a crystalline domain aligned with a pre-defined pattern.[203] A well-known template in anodic aluminum oxide (AAO) with a channel size of 10 nm to 10 μm, which directs the CPs to be coated normally to the AAO pores.[59,203]

In oCVD, the deposition temperature has been used for crystallinity control.[140] It was also observed that acid rinsing aids the broadening of the crystallographic signature and also intensifies it, which was attributed to a higher degree of crystallinity.[136] The relationship between deposition temperature and post-processing to crystallinity remains to be understood. The crystallinity also depends on the regioregularity which could not be controlled by oCVD as mentioned before.

ii. Packing. In addition to intra-chain charge transfer as the dominant mechanism of conductivity, charge carriers need to hop in between CP chains, a mechanism that is known as inter-chain conductivity.[204] For this purpose, the lower the distance between the chains, the easier this hopping occurs. This topic is understood as the packing of CP chains.

It was mentioned before that for the sake of solubility, long side chains – often alkyl – are introduced in the polymer structure. Generally speaking, such a modification undermines a close π–π stacking between planes of CP chains as a result of possible plane torsion. In this regard, for alkylated CPs, the best packing is obtained when these side chains are so-called interdigitated (Fig. 7(b) *vs.* Fig. 7(c)).[205,206] The interdigitization tendency is favored for the case of linear alkyl chains rather than branched structures.[160,192,207]

Also, a related but different aspect of thin-film conductivity is their spatial conformation relative to an underlying substrate. This is due to the anisotropic nature of charge transfer in randomly oriented CP chains. An isotropic charge transfer of either in-plane or out-of-plane charge transfer might be preferred in different applications. For example, in the case of a field-effect transistor, since the direction of charge mobility is horizontal, an edge-on to the substrate (in-plane π stacking) is desired; while for OPVs with vertical charge mobility, a face-on CPs orientation (out-of-plane π stacking) is preferred.[208] In this regard, research was done to shed light on the morphology control of CPs in order to stimulate the face-on and edge-on orientation of polymeric chains relative to the substrate (Fig. 7(d)).[209]

A relevant but different aspect is the coplanarity of CP chains: Chen *et al.* reported a systematic study of isoindigo-based polymers with increased polymer planarity by substituting thiophenes for phenyl rings and investigated how this structural modification impact polymer orientation toward silicon-based substrates. They concluded that in case the obtained polymer is soluble, interpolymer interaction is minimized and the van der Waals interaction between the polymer and the substrate is encouraged, favoring a face-on orientation of the synthesized CPs. However, for a less planar polymer (more chain twisting), the chains are more aggregated, resulting in favored edge-on orientation upon deposition.[208] Mullen *et al.* copolymerized five different benzodithiophene isomers with alkylated dithiophene and observed that an increased degree of curvature (monomer angle between 106° and 180°) decreased ordering of chains and packing in their associated solid films.[210] Consequently, although smaller curvature angles could prompt packing, the authors advise an intermediate level of curvature to preserve solubility as it was observed that molecules with the lowest degree of curvature were difficult to process. This indeed could be a potential opportunity for oCVD.[210]

The attempts for orientation control of CPs from the solution phase on a substrate have been followed in three different strategies:[211]

(i) By using shear forces including frictional transfer, mechanical rubbing, roller transfer, and strain alignment.

(ii) Fine-tuning of solution properties to prompt certain orientation: methods include the use of certain coating

techniques such as dip coating, blade coating, solution shearing,[212] wire-bar coating which have shown the ability to "guide" polymer chains for a certain orientation. Also, off-center spin coating, floating film-transfer method, and directional solvent evaporation could be included in this topic.

(iii) Substrate-directed CP ordering: for which epitaxial crystallization and dynamic template-directed orientation.

The details for each of these strategies and techniques are available in the literature[59,60,211–213] and we do not discuss them here. The important point is except for the second strategy which exploits the possibilities with different solution processing methods to obtain the desired orientation, both the first and third strategies could be benefited by oCVD methodology. Yet, it is worth mentioning that not all of the above methods are easily translatable to scale-up and large-area processing. In addition, most of them are not applicable in multi-layer and device-relevant manufacturing as they will result in either chemical or mechanical damage to the other layers.[211]

There is less information in oCVD on CP and their packing control. A well-studied case is PEDOT deposition using $FeCl_3$, which showed a transition from edge-on to face-on orientation when the deposition temperature was increased from a lower temperature to 300 °C. The oCVD-grown PEDOT with face-on orientation in this case was associated with a record conductivity above 6000 S cm^{-1}. With the motivation of lowering the deposition temperature, the same research group reported that by using $VOCl_3$ as an oxidant, it was possible to obtain pure face-on orientation at a deposition temperature as low as 140 °C. However, in the latter case, the conductivity was lower (2800 S cm^{-1}).[140,214] From a post-processing point of view, PEDOT film rinsing with HBr showed to improve packing.[136]

d. Doping (and oxidants)

Doping is the process that offers the conjugated polymers the conductivity they are known for. It is achieved by the incorporation of a small quantity of a chemical that lowers the resistivity of a CP. There could be three types of dopants, namely: inorganic, organic, and polymeric.[19]

Most of the inorganic compounds used as dopants for CPs are gaseous molecules (*e.g.*, halogens, oxygen), metals (*e.g.*, Li, Na, Mg), Lewis acids (*e.g.* $FeCl_3$, $SbCl_5$, $VOCl_3$), and inorganic acids (*e.g.* HCl, H_2SO_4). Although the oxidizing nature of a dopant determines doping efficiency, an important consideration regarding inorganic dopants is that they are the smallest among different types of doping compounds. This results in a higher mobility of their counter ions within a polymeric network and consequently higher conductivity.[19] In solution processing, a challenge for inorganic dopants has been their processability with common solvents. CPs are hydrophobic in nature and inorganic dopants are hydrophilic, making it difficult to find a common solvent.

To overcome the solubility limitation of inorganic dopants, one approach was using organic dopants which are hydrophobic as well. It could also help with better environmental stability of CPs oxidation in an ambient environment. However, they have comparably bigger counter ions which restrict their mobility in CPs and lower the conductivity. Some examples of organic dopants include sulfonate derivatives of anthraquinone or naphthalene, acetic, citric, oxalic, and tartaric acid, and copper phthalocyanine. Obviously, polymeric dopants offer the biggest size of compounds in the above classification, though the most stable one. Examples are polyaniline doped with polyacrylic acid and PEDOT doped with PSS.[19]

Another perspective is how the interaction between the dopant and CP impacts its microstructure. Ma *et al.* reported that by using an organic molecule (N-DMBI) for doping of n-type CP (FDBPPV), better carrier mobility was achieved by enhancing molecular packing.[215] Another example is PEDOT with preferential edge-on orientation when doped with PSS, Tos, or OTf,[216–220] while favoring face-on orientation when doped with smaller counter ions (like chloride Cl^-).[52,140]

Although there is no limitation in exploiting different doping agents in the oCVD method, it generally was not a center of attention and only a fraction of the dopants are used for synthesis in practice. It should be noted that in oCVD, the same oxidant that is used for synthesis would remain in the polymer structure and serve as a dopant. Possibly a post-processing step could be added to improve the properties with the aid of a second oxidizing agent, as reported in the case of PEDOT.[140]

On the other hand, it is safe to conclude that the solvent incompatibility for inorganic dopants with CPs is resolved by oCVD. Along with the superior performance of inorganic dopants, this might be the reason that $FeCl_3$[65] has been widely used as a dopant in oCVD of CPs. Other dopants used are as follows: Br_2,[176,221] $CuCl_2$,[102,222] $VOCl_3$,[125,223] $SbCl_5$,[125,174,223,224] $MOCl_5$[225] and H_2SO_4.[150]

5. Polymer–substrate interface

An important aspect of surface coating is how the deposited coating interacts with the underlying substrate. Such an interaction not only contributes to the functionality of the top layer but is also important for the long-term stability of the coating. Below, we review the most relevant aspects of coating–substrate interfacial properties from the viewpoint of CPs and oCVD.

a. Uniformity

Uniformity is a critical aspect of coating CPs on a surface. The processing history of the coating along with the polymer–substrate interaction determines the thin film uniformity of a specific polymer–substrate pair. CVD methods in general are well-recognized to result in outstanding uniformity compared to solution-processed thin film coatings.[67] The reasons could be understood in a number of limitations that solution coating techniques suffer when compared to solvent-free techniques, which of course may be different for each specific wet method. For example, drop casting, while being an easy method, is negatively influenced by the "coffee ring effect". When the solvent evaporation rate is higher at the edge of the droplets

compared with its center, it results in a non-uniform film.[226,227] Spin coating on the other hand has been able to give highly uniform films compared to drop-casting or other wet-processing techniques and as a result has often been the method of choice.[228,229] However, during the drying stage, the solution gradually becomes more viscous and the coating enters a so-called shrinkage stage. This sometimes results in the formation of meniscus and film thinning at the side walls. On the other hand, spin coating fails to result in high-ordered conjugated thin films as the solvent usually evaporates too fast and does not allow enough relaxation time to the polymeric chain ordering. To partially compensate for this problem, high boiling point solvents could be used.[205] However, this could end in residual solvents trapping in the coating microstructure, up to 20%.[230] It has been reported that this could be mostly resolved by exposing the film to high temperatures (annealing).[231] Yet even with annealing, the residual solvent negatively affects the film properties and this may be exacerbated by using high boiling point chlorinated solvents, which are not a favorable choice for the environment.[199]

b. Conformality

Conformality refers to how a thin film homogeneously covers or "shrink wraps" on a surface. A surface could be qualitatively categorized into smooth and rough. Rough in here stands for nano/micro-structured surfaces which have a texture and/or 3D structure. Two modes of coverage are conformal and planar.[232]

Conformal coverage features a film with uniform thickness resembling the geometry of the underneath substrate. This type of coverage is challenging for solution processing primarily because of surface tension effects.[233,234] This is particularly a limitation for textured surfaces due to dewetting.[235] Solution processing may result in surface bridges inhibiting the liquid to penetrate the porous three-dimensional features of the geometry.[232] For example, spin coating as a highly exploited method, is controlled by two driving forces when coating a surface: centrifugal and capillary.[236] In case a geometry has 3D features, centrifugal force tries to "push" the solution into the 3D network and make the film conformal; while the capillary forces want to make the flow level. In the beginning, the centrifugal forces are the main driving force; however, as the solvent evaporates and the solution becomes more viscous, the capillary forces dominate.[236]

CVD on the other hand is widely known to result in conformal coverage on different surfaces including porous 3D surfaces.[125,232] This is the result of a number of factors. First, from a mass transport point of view, vapors have several orders of magnitude higher diffusion coefficients than liquids. This means that in the case of a 3D geometry, vapors could better diffuse into the surface sites which are not easily accessible for liquids. Additionally, the surface adsorption of gaseous molecules is much lower than the solution in a single "collision" with the substrate. This results in a slower morphology development and as a result higher relaxation time of the polymer chains that favors conformal coverage. Finally, in CVD practice in general, the tendency of any surface spot to be coated would gradually decrease upon film formation. This feature is called "self-limiting surface reaction" and contributes to conformality, which could be imagined as the opposite of capillary levelling in solution processing.[233] Fig. 8(a) shows a porous textile that is coated with PEDOT:PSS solution using spin

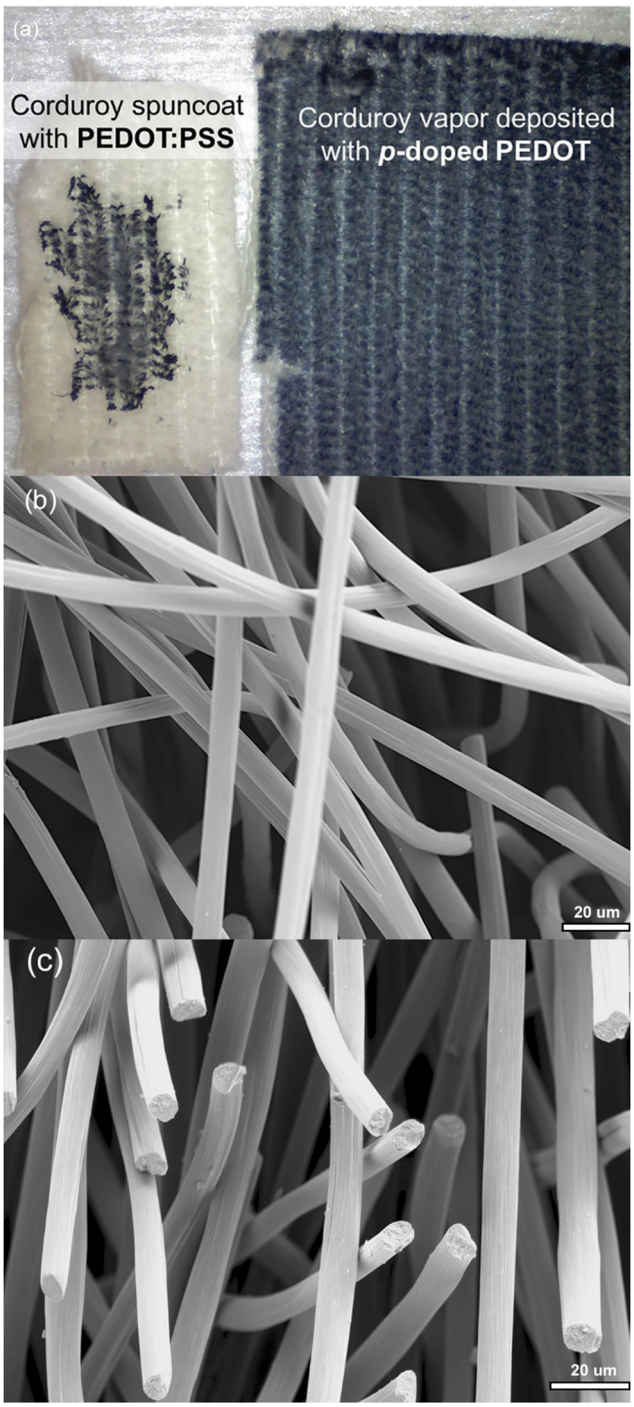

Fig. 8 (a) Corduroy swatch with 2 in^2 surface coated with PEDOT: PSS solution (left) and with 4 in^2 surface deposited with PEDOT *via* oCVD; reproduced from ref. 103 with permission from The Royal Society of Chemistry. (b) and (c) Microporous carbon felt uncoated and coated with PPy *via* oCVD, respectively.[237]

coating, resulting in poor uniformity and conformality, as well as coated substrate using oCVD resulted in highly uniform and conformal PEDOT films.[103] In the same manner, Fig. 8(b) and (c) shows uncoated and PPy-coated microporous carbon felt.[237]

c. Interfacial adhesion

As a practical aspect, it is necessary for a CP film to firmly adhere to the underlying substrate during the lifespan of the relevant application. Here, adhesive strength is the work required to separate a CP film from its substrate.[238] Therefore, the bonding strength between the film and the substrate determines the force of adhesion, the failure of which is a result of extrinsic and/or intrinsic stresses.[239] Extrinsic stresses, by definition, arise from external sources such as UV irradiation, chemical oxidation, mechanical stress *etc.* On the other hand, intrinsic stresses are a result of the interfacial features of any substrate-thin film pairs which are determined by the nature of thin film/substrate on the one hand and the history of thin film formation on the other hand, which are all affected by surface wetting behavior, thermodynamic work of adhesion, and interfacial tension.[238,239] These intrinsic aspects could be further affected by extrinsic stresses as well. Relevant discussion in this review is how oCVD differs from solution processing at the film–substrate interfacial adhesion from the intrinsic point of view. To discuss this, we briefly discuss about physical or chemical bonding.

i. Physical bonding. In physical bonding, the adhesion force is mainly determined by the bonding surface area and interfacial tension.[238] Intuitively, when there is a higher surface area between a CP and a substrate, it results in a more intimate contact between the two,[238] which could be further supported by van der Waals and electrostatic forces. This is a specially the case for textured, porous and 3D substrates, which all offer increased surface area. An example is when the indium tin oxide surface was roughened to improve the adhesion of poly(3,4-propylenedioxythiophene) (PProDOT) through so-called ''mechanical interlocking''.[240,241] However, there is a potential drawback that the textured surface counterproductively results in decreased adhesion as a result of uncoated areas, which are left behind as voids.[238] In principle, both solution coating and oCVD-coated CP could benefit from such a surface effect. However, oCVD could possibly outperform solution processing for 3D substrates because of all the challenges solution processing faces, which are discussed in the previous two sections.

Next comes the interfacial tension between a CP film and a substrate. The adhesive force is maximum when the difference between the surface free energy of the film and the substrate (called interfacial tension) is minimum.[238] This surface tension is formed during the coating process, the control of which is crucial for adhesion. Therefore, a CP film on polymeric substrate results in a lower surface tension than a CP/metal pair. This aspect is the same for both oCVD and solution coating. However, for any two layers, the process by which they come into contact will determine the level of internal stress. This will be the source of interfacial failure upon exposure to external stresses over time. For example, if there is mechanical compressive stress, the film is susceptible to delamination or cracking in case of tensile stress.[239,242,243]

During solution processing, the solvent evaporates, and the polymeric film has to shrink. However, the polymer at the solid–liquid interface is already physically adhered to the substrate. As a result, it could not ''flow'' in parallel with the volume change.

Therefore, polymer chains are locked in configurations that are thermodynamically unfavorable,[244–246] which causes internal stress in the plane of the coating.[247] Additionally, the physical mismatch between a polymer and a potential metallic substrate prompts interfacial failure during time as a result of different responses to external stresses.[248]

In polymer CVD practice, there is no report addressing the phenomenon of internal stress. However, from the inorganic CVD process, it is well known that internal stresses would form as a result of non-equilibrium deposition conditions.[249] The mechanism is such that the first adsorbed molecules on a substrate occupy the spots that do not possess the lowest energy, which is then trapped by the new incoming molecules resulting in internal stress. Such a process could be partially controlled by the deposition rate.[239] At the time of writing this review, a systematic study comparing the degree of internal stress during polymer oCVD and solution processing is missing. Therefore, further comparison is not possible.

ii. Chemical bonding. The other adhesion force arises when a polymer forms chemical bonds with a substrate. Compared with the physical bonding, these thin films are more robust at the interface.[250,251] Chemical bonds between CPs and substrates are pursued by both solution processing and CVD methods using the terms of polymer-grafted or polymer-linked substrates. There are two methods of grafting between a substrate and a polymeric layer, either grafting-to or grafting-from.

In solution processing, different surface-initiated polycondensation methods have been exploited to prepare well-defined conjugated polymer brushes. This is a bottom-up approach that results in CP grafting from a substrate.[252] The other method is when an already developed polymer chain is grafted to a surface. In an example, the cyclopentadiene–maleimide Diels–Alder ligation was used to graft poly(3-hexylthiophene) to a pre-treated silicon substrate.[253]

In oCVD, inspired by the work of Kovacic,[254] it was observed that when a substrate has aromatic groups in its structure, EDOT makes a chemical bond with the substrate, following the proposed mechanism (Scheme 3).[255] In another report, a simple and straightforward procedure, (3-aminopropyl) trimethoxy silane[129] was attached to a silicon wafer forming Si–O–Si, and the molecule was used as a linker to PPy. Using the same principles, linker molecules such as 4-aminothiophenol, methyl 4-mercaptobenzoate, or 4-mercaptobenzoic acid were used as a linker molecule to graft poly(EDOT-*co*-3-TE) and poly(EDOT-*co*-TAA) grown by oCVD.[145] These methods could be compared with a grafting-to approach in solution processing. Unlike solution processing, the grafting-from approach has not been replicated in oCVD yet.

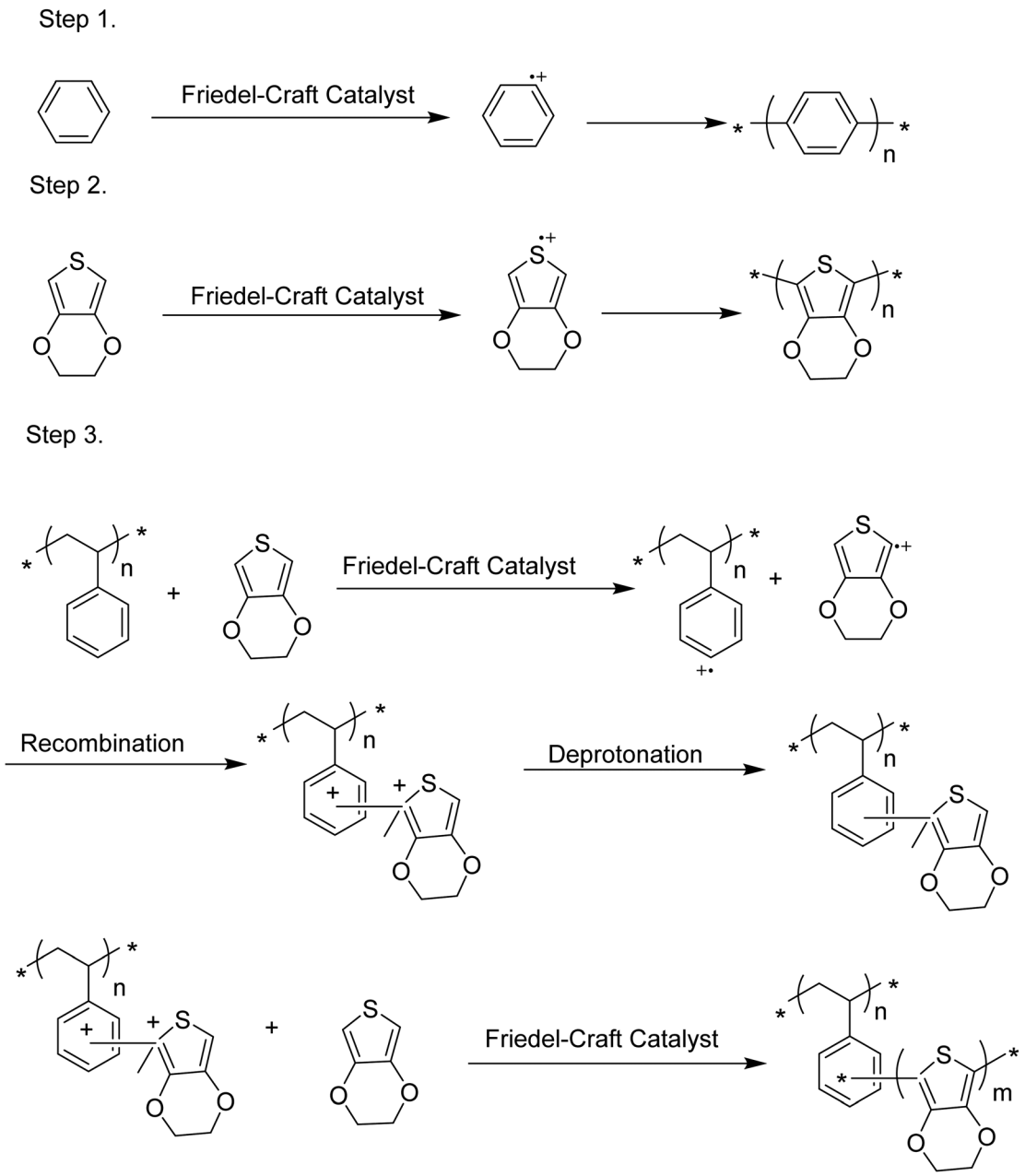

Scheme 3 The proposed mechanism of PEDOT grafting to a substrate having aromatic groups in its structure.[255]

iii. Polymer properties. In addition to the interfacial bonding of CP films and a substrate, polymer cohesive forces affect the interfacial adhesion as well.[256] More specifically, higher polymer chain entanglement (which depends on its M_w) results in higher cohesive forces of these chains,[257] which could act as a ''support'' for an interfacial domain of the CP film, providing a more robust contact.

6. Substrates

The wide variety of substrates that could be used in CVD processing is probably one of the most outstanding features it offers. Discussion on substrates may be conducted in three directions, namely (i) the substrate surface geometry, (ii) the substrate material and (iii) processing concerns.

As a solvent-free procedure, oCVD provides the opportunity for thin film deposition of CPs on a diverse range of substrate materials and surface geometries. Examples are the reports by Wang *et al.*[145], describing a methanol sensor development using printed circuit boards as the substrate and coated with poly(3,4-ethylenedioxythiopheneco-thiophene-3-aceticacid) [poly(EDOT-*co*-TAA)] and/or poly((3,4-ehylenedioxythiophene-*co*-thiophene-3-ethanol) ethanol) [poly(EDOT-*co*-3TE)]. Smolin *et al.* used micro/mesoporous carbide-derived carbon (CDC) and porous Mo_2C CDC as substrates and coated them with

Table 2 The variety of substrates used for deposition of conjugated polymers along with their applications

Substrate	Applications	Polymer	Ref.
Cotton towel/corduroy fabric	Wearable electronics	P(DMT)	103,149
Printed circuit boards	Methanol sensor	Poly(EDOT-*co*-TAA)	145
Electro-spun mat	Chemiresistive biosensor	Poly(EDOT-*co*-3TE)	146
Porous CDC/Mo_2C CDC	Energy storage	PANI	174,224
Unmodified paper	Organic photovoltaic	PEDOT	131
Graphene	Organic solar cell	PEDOT	132
Aligned carbon nanotube	Energy storage, sensor	PEDOT	133,134
n-doped ZnO layer	Organic optoelectronic	PEDOT, PPy	135,269
Cellulose filter paper/porous nylon membrane	Supercapacitor	PEDOT	138
Sponge-type carbon felt	Electrocatalytic system	Polydopamine	150
Porous AAO/TiO_2/activated carbon	Energy storage	PT	125
Microporous polyurethane fibers	Piezoresistive sensor	PPy	44

PANI for energy storage applications.[174,224] In another example, Nejati *et al.* deposited PANI onto nanostructured AAO, titanium oxide, and activated carbon and used the composite for energy storage applications with enhanced properties in performance. Their result showed that the ultrathin coating of PANI could adhere to the underlying nanostructure surface, which ensures a high surface area that is crucial for the specific application.[125] Furthermore, the possibility of coating an ultrathin layer in the order of 4 nm could significantly add to the long-term stability of the modified electrode.[125,258] Exploiting the possibility to coat a textured substrate with nano/meso/micro features with a CP and preserve its geometry has shown to be a versatile approach for improved performance across a wide range of applications. For example, Kim *et al.* deposited 20 nm of PEDOT on mesoporous ITO and validated it as a Pt-free cathode for application in dye-sensitized solar cells (DSSCs) with a performance similar to a Pt-based cathode.[259] In another example Howden *et al.* grew PEDOT by oCVD on a range of macro/nano-scale textured surfaces and demonstrated that this procedure increased light absorption in photovoltaics by different light trapping mechanisms.[260] Conformal PEDOT layer of 8 to 17 nm on vertically aligned carbon nanotube (VA-CNT) showed a 10-fold increased sensitivity for volatile organic compound (VOC) sensing application.[134] Depositing of 10 nm of PEDOT on VA-CNT showed also showed a 10-fold increase in pseudocapacitance when the hybrid material was used as a supercapacitive electrode.[133]

The oCVD method is generally categorized as a substrate-independent method due to the possibility of using a diverse range of materials and surface features, as mentioned above.[66,141–143] This substrate-independence of oCVD is especially beneficial in a wide range of CPs applications, where multiple layers are successively deposited. In these cases, the interaction of solvent with all the layers underneath becomes relevant. In this regard, one important concern is that the step of depositing a subsequent layer should not damage the pre-existing layer. This is achieved by choosing orthogonal solvents in device fabrication using wet processing.[261]

On merit of oCVD, PEDOT was deposited on both sides of a porous paper and the composite material was tested for its supercapacitive performance and flexible energy storage application.[138] The same strategy was used to fabricate flexible paper-based organic photovoltaics.[131] Also, a convenient wearable electronic device could be fabrics/textiles due to their widespread use in daily life. Yet such materials are susceptible to deformation and damage when in contact with solvents.[262] On the other hand, oCVD proved to be a feasible method for depositing conjugated polymers for different applications for sensitive substrates.[263] Andrew *et al.* reported employing different types of textiles as substrates for deposition of conjugated polymers across different applications such as supercapacitors, optoelectronic, transistors, and sensors.[157,264–267] The same research group also reported depositing PProDOT on microtextured living plants for health monitoring applications, which takes research in this area to the next level.[268] A list of substrates reported in the literature for oCVD is provided in Table 2 along with their proposed applications.

Despite the benefits oCVD provides in substrate choice, it is recognized that in one case oCVD is not substrate-independent and that is when the oxidant reacts with the substrate. In some of these cases, surface cationic species are formed which could provide the opportunity for covalent linking and hence improve the interfacial adhesion of the coating.[65] Yet, given that strong oxidants are used in synthesis of conjugated polymers, the possibility for surface degradation of vulnerable substrates such as polymers could not be excluded. In fact, the interaction of metal halides including $FeCl_3$ (as the most common oxidant so far) with a number of polymers such as nylon or PVC is well documented decades ago.[270,271] It is necessary for future research on oCVD to take into account any possible substrate deterioration during synthesis especially for more fragile materials including polymers, a topic that is mostly overlooked until now.

7. Industrialization and scale-up

As a milestone in oCVD development, an initial scale-up attempt was reported in 2015.[272] PEDOT was successfully deposited on larger than usual areas of $\sim 20 \times 30$ cm^2 textile/PET foil for the first time. The oCVD process was adopted in the roll-to-roll (R2R) processing procedure considering its industrial relevance (Fig. 9(a)). Oxidant and monomer are vaporized

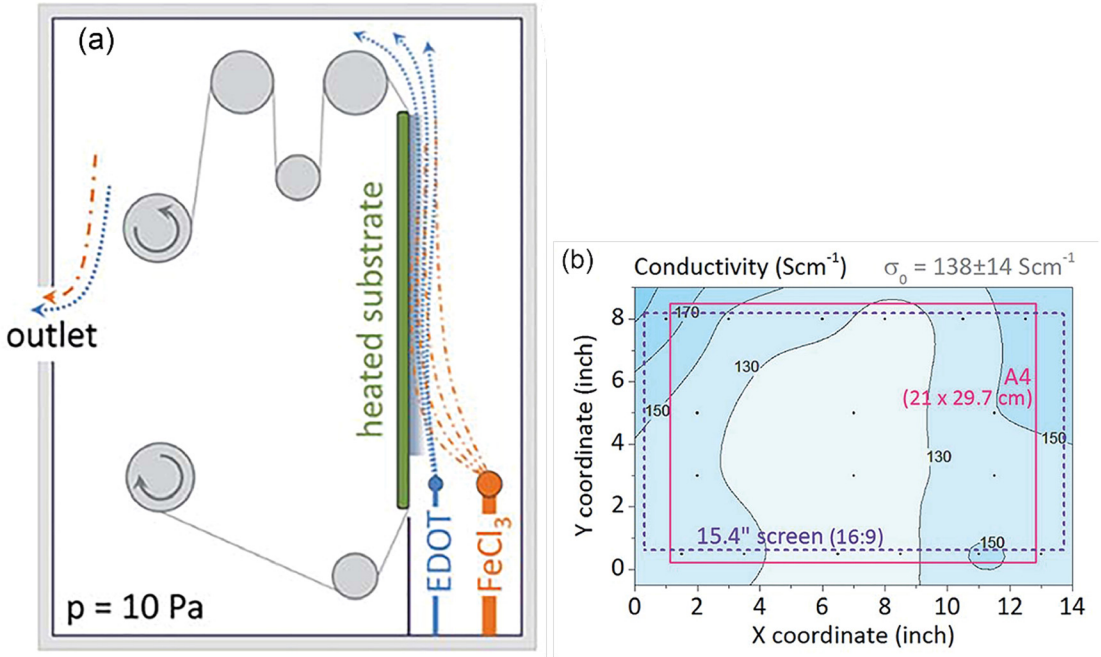

Fig. 9 (a) An illustration of the R2R oCVD reactor constructed in MIT; (b) PEDOT conductivity distribution deposited in an area of ~20 cm × 30 cm at a deposition temperature of 100 °C. Reproduced from ref. 272 with permission from The Royal Society of Chemistry.

and directed onto the surface in a vertical manner with an angle of 0°. The rolling helps with uniformity of thin film deposition on the substrate. Uniformity of PEDOT characteristics was monitored by the change in film conductivity on different areas of ~ an A4-sized PET foil. The result showed a standard deviation of up to 10% in conductivity values (Fig. 9(b)).[272] The above result provides an initial indication of the oCVD success for scaling up.

However, there are certain aspects that are not yet understood. One primary aspect is batch-to-batch variation between the synthesized polymers using oCVD, which is a critical aspect for the commercialization of any chemical process in terms of process reliability.[273,274] This aspect becomes particularly pressing considering that as a step-growth polymerization technique, oxidative polymerization is inherently not a controlled procedure, giving rise to batch-to-batch variance.[275] To address this in the field of CPs, controlled chain-growth polymerization has been proposed which could successfully control the polymerization kinetics. These reactions again get the advantage of catalysts in their synthesis.[276,277] In this regard, it looks absolutely necessary to work toward catalytic chemical vapor deposition reactions of CPs, possibly by getting inspiration from the field of inorganic semiconductors. An immediate idea could be the deposition of a thin catalyst layer on a substrate to enhance the chemical environment and further exploit the layer as a substrate.[278]

Another aspect worth noting is recording and ultimately modelling the deposition rate of CPs grown by oCVD. Within the chemical vapor deposition community, it is well known and documented that relative concentration of precursors, deposition temperature, and vacuum pressure could also be used to fine-tune film growth temperature.[279,280] Also, the fluid dynamics of the reaction environment which is associated with reactor size and configuration as well as flow channels all play a role. For industrial adaptation, it is crucial to record, quantify and model these aspects. Such an endeavor has been followed in the inorganic CVD field (which has long been adopted in industry) and to a good extent for initiated chemical vapor deposition of polymers.[281,282] Yet, it is apparent that for oCVD, this has yet to be developed. For this purpose, a good start could be a systematic inclusion of deposition rate data along with reactor configurational features. Reviewing the literature, it could be concluded that such data exists for some reports, yet is not included in many reports.

8. Future perspective and concluding remarks

The oCVD process is reviewed and compared with solution-based techniques for synthesis and film formation of conjugated polymers. As a synthesis method, oCVD offers the possibility of direct polymerization of the most common conjugated monomers without any additional step to modify the monomer. Yet, compared to solution-based techniques, it is limited in terms of monomer versatility as it does not have the freedom of using a catalyst to facilitate the polymerization of certain conjugated monomers as well as the challenges arising from the inherent vapor pressure properties of certain monomers. Solvent-based techniques on the other hand accommodate more diverse synthesis routes, which makes it possible to control the structure–property relationship of CPs to a greater

extent. Solvent-based techniques also offer bulk synthesis of CPs as well as the diversity in their chemical structure, which might be at the cost of cumbersome synthesis routes.

In terms of processing and thin film formation, oCVD generally outperforms solvent-based coating techniques as it offers the possibility of producing highly uniform, conformal, and robust CP films with good control over thickness and over a diverse range of substrates (planar or with a 3D texture). On the other hand, solvent-based coating methods offer versatility, economic feasibility, and technological maturity, which give rise to their ease of adaptation in industrial settings. Yet solvent-based techniques face challenges when precision coating on non-planar and textured surfaces is required, combined with the inherent insolubility issue related to conjugated polymer chemistry.

Future research should be aimed at widening the ''monomer library'' of the oCVD method, which might become possible by the adaptation of new polymerization mechanisms with the aid of catalysts or photo-induced processes, details of which were introduced in the current review. Also, attempts should be made to overcome synthesis challenges arising from low vapor pressure of certain conjugated monomers. This could be possibly by use of a new generation of high-temperature oCVD reactors, derived from inorganic CVD practice. Additionally, investigation of thin film properties in terms of microstructure could significantly contribute to the film performance of the CPs produced by oCVD and pave the way for their adaptation for device fabrication.

Conflicts of interest

The authors have no conflicts to declare.

Notes and references

1 J. Mort, *Science*, 1979, **1980**(208), 819–825.
2 F. Lincoln Vogel, *Synth. Met.*, 1979, **1**, 1.
3 **https://www.oxfordreference.com/**.
4 E. P. T. Kerja, *Conducting Polymers: A New Era in Electrochemistry*, 1967, vol. 13.
5 M. Kraft, S. Adamczyk, A. Polywka, K. Zilberberg, C. Weijtens, J. Meyer, P. Görrn, T. Riedl and U. Scherf, *ACS Appl. Mater. Interfaces*, 2014, **6**, 11758–11765.
6 N. Casado and D. Mecerreyes, *RSC Polym. Chem. Ser.*, 2021, 1–26.
7 R. Schroot, M. Jäger and U. S. Schubert, *Chem. Soc. Rev.*, 2017, **46**, 2754–2798.
8 F. Szillat, B. V. K. J. Schmidt, A. Hubert, C. Barner-Kowollik and H. Ritter, *Macromol. Rapid Commun.*, 2014, **35**, 1293–1300.
9 G. Inzelt, *Conducting Polymers A New Era in Electrochemistry*, Springer-Verlag, Berlin Heidelberg, 2008.
10 J. Kim, J. H. Kim and K. Ariga, *Joule*, 2017, **1**, 739–768.
11 D. A. Buttry and F. C. Anson, *J. Electroanal. Chem.*, 1981, **130**, 333–338.
12 O. Inganläs, *Chem. Soc. Rev.*, 2010, **39**, 2633–2642.
13 Y. Nagasaki, *Polym. J.*, 2018, **50**, 821–836.
14 A. Dianatdar, O. Akin, I. Mongatti, J. Momand, G. Ruggeri, F. Picchioni and R. K. Bose, *RSC Adv.*, 2021, **11**, 35187–35196.
15 A. McNaught and A. D. Wilkinson, *The IUPAC Compendium of Chemical Terminology*, International Union of Pure and Applied Chemistry (IUPAC), Research Triangle Park, NC, 2019.
16 H. Shirakawa, E. J. Louis, A. G. MacDiarmid, C. K. Chiang and A. J. Heeger, *J. Chem. Soc., Chem. Commun.*, 1977, 578–580.
17 Editorial, *Nat. Mater.*, 2020, **19**, 921.
18 W. Deits, P. Cukor, M. Rubner and H. Jopson, *Synth. Met.*, 1982, **4**(3), 199–210.
19 P. Kar, *Doping in Conjugated Polymers*, John Wiley & Sons, Inc., Scrivener Publishing LLC, Hoboken, New Jersey, Salem, Massachusetts, 2013.
20 A. J. Heeger, *Chem. Soc. Rev.*, 2010, **39**, 2354–2371.
21 A. Dianatdar, M. Miola, O. De Luca, P. Rudolf, F. Picchioni and R. Bose, *J. Mater. Chem. C*, 2022, **10**, 557–570.
22 J. Heinze, Electronically conducting polymers, in *Electrochemistry IV. Topics in Current Chemistry*, ed. E. Steckhan, 1990, vol. 152, pp.1–47.
23 J. R. Skotheim, T. A. Elsenbaumer and R. L. Reynolds, *Handbook of Conducting Polymers*, Marcel Dekker, Inc, New York, NY, USA, 1998.
24 T. Onggar, I. Kruppke and C. Cherif, *Polymers*, 2020, **12**, 1–46.
25 R. S. Potember, R. C. Hoffman, H. S. Hu, J. E. Cocchiaro, C. A. Viands, R. A. Murphy and T. O. Poehler, *Polymer*, 1987, **28**, 574–580.
26 T. Yokozawa and Y. Ohta, in *Semiconducting Polymers: Controlled Synthesis and Microstructure*, ed. C. Luscombe, The Royal Society of Chemistry, 2016, pp.1–37.
27 J. Pecher and S. Mecking, *Chem. Rev.*, 2010, **110**, 6260–6279.
28 E. F. Woods, A. J. Berl and J. A. Kalow, *ChemPhotoChem*, 2021, **5**, 4–11.
29 R. K. Sadhir and K. F. Schoch, *Thin Solid Films*, 1993, **223**, 154–160.
30 D. Bilger, S. Z. Homayounfar and T. L. Andrew, *J. Mater. Chem. C*, 2019, **7**, 7159–7174.
31 M. Wan, *Conducting Polymers with Micro or Nanometer Structure*, Tsinghua University Press, Berlin, Beijing, 2008.
32 J. M. D'Arcy, H. D. Tran, V. C. Tung, A. K. Tucker-Schwartz, R. P. Wong, Y. Yang and R. B. Kaner, *Proc. Natl. Acad. Sci. U. S. A.*, 2010, **107**, 19673–19678.
33 T. Yamamoto, T. Yokozawa, I. Osaka, R. D. McCullough, J. Liu, J. W. Y. Lam, B. Z. Tang, Y. Morisaki, Y. Chujo, M. Takase, M. Iyoda, A. Nagai, P. W. Siu, D. P. Gates, K. Naka, A. Wild, A. Winter, M. D. Hager, U. S. Schubert and K. Akagi, *Conjugated Polymer Synthesis: Methods and Reactions*, WILEY-VCH Verlag & Co. KGaA, Weinheim, Germany, 2010.
34 A. Mohammadi, M. Hasan, B. Liedberg and I. Lundstrom, *Synth. Met.*, 1986, **14**, 189–197.

35 J. P. Lock, S. G. Im and K. K. Gleason, *Macromolecules*, 2006, **39**, 5326–5329.
36 L. Dou, Y. Liu, Z. Hong, G. Li and Y. Yang, *Chem. Rev.*, 2015, **115**, 12633–12665.
37 O. Ostroverkhova, *Chem. Rev.*, 2016, **116**, 13279–13412.
38 J. F. Mike and J. L. Lutkenhaus, *J. Polym. Sci., Part B: Polym. Phys.*, 2013, **51**, 468–480.
39 A. C. Grimsdale, K. L. Chan, R. E. Martin, P. G. Jokisz and A. B. Holmes, *Chem. Rev.*, 2009, **109**, 897–1091.
40 S. Ghosh and R. N. Basu, *Conjugated Polym. Nanostruct. Energy Convers. Storage Appl.*, 2021, 207–232.
41 T. Nezakati, A. Seifalian, A. Tan and A. M. Seifalian, *Chem. Rev.*, 2018, **118**, 6766–6843.
42 C. Zhu, L. Liu, Q. Yang, F. Lv and S. Wang, *Chem. Rev.*, 2012, **112**, 4687–4735.
43 E. Smela, *Adv. Mater.*, 2003, **15**, 481–494.
44 A. Mukherjee, A. Dianatdar, M. Z. Gładysz, H. Hemmatpour, M. Hendriksen, P. Rudolf, M. K. Włodarczyk-Biegun, M. Kamperman, A. G. Prakash Kottapalli and R. K. Bose, *ACS Appl. Mater. Interfaces*, 2023, **15**, 31899–31916.
45 M. F. De Riccardis, *Fundam. Conjugated Polym. Blends, Copolym. Compos.*, 2015, 519–579.
46 P. P. Deshpande, N. G. Jadhav, V. J. Gelling and D. Sazou, *J. Coat. Technol. Res.*, 2014, **11**, 473–494.
47 M. Ates, *J. Adhes. Sci. Technol.*, 2016, **30**, 1510–1536.
48 L. Allison, S. Hoxie and T. L. Andrew, *Chem. Commun.*, 2017, **53**, 7182–7193.
49 M. Sairam, S. K. Nataraj, T. M. Aminabhavi, S. Roy and C. D. Madhusoodana, *Sep. Purif. Rev.*, 2006, **35**, 249–283.
50 P. Lindemann, M. Tsotsalas, S. Shishatskiy, V. Abetz, P. Krolla-Sidenstein, C. Azucena, L. Monnereau, A. Beyer, A. Gölzhäuser, V. Mugnaini, H. Gliemann, S. Bräse and C. Wöll, *Chem. Mater.*, 2014, **26**, 7189–7193.
51 G. Zhang, Z. A. Lan and X. Wang, *Angew. Chem., Int. Ed.*, 2016, **55**, 15712–15727.
52 M. Heydari Gharahcheshmeh and K. K. Gleason, *Mater. Today Adv.*, 2020, **8**, 100086.
53 M. Armand, *Adv. Mater.*, 1990, **2**, 278–286.
54 J. A. Shetzline and S. E. Creager, *J. Electrochem. Soc.*, 2014, **161**, H917–H923.
55 Z. Qiu, B. A. G. Hammer and K. Müllen, *Prog. Polym. Sci.*, 2020, **100**, 101179.
56 M. H. Harun, E. Saion, A. Kassim, N. Yahya and E. Mahmud, *Sensors*, 2007, **2**, 63–68.
57 T. H. Le, Y. Kim and H. Yoon, *Polymers*, 2017, **9**, 150.
58 M. G. Sumdani, M. R. Islam, A. N. A. Yahaya and S. I. Safie, *Polym. Eng. Sci.*, 2022, **62**, 269–303.
59 L. Zhai, S. I. Khondaker, J. Thomas, C. Shen and M. McInnis, *Nano Today*, 2014, **9**, 705–721.
60 M. Chang, G. T. Lim, B. Park and E. Reichmanis, *Polymers*, 2017, **9**, 23–31.
61 C. I. Awuzie, *Mater. Today: Proc.*, 2017, **4**, 5721–5726.
62 K. Namsheer and C. S. Rout, *RSC Adv.*, 2021, **11**, 5659–5697.
63 R. J. Waltman and J. Bargon, *Can. J. Chem.*, 1986, **64**, 76–95.
64 J. Heinze, B. A. Frontana-Uribe and S. Ludwigs, *Chem. Rev.*, 2010, **110**, 4724–4771.
65 M. Heydari Gharahcheshmeh and K. K. Gleason, *Adv. Mater. Interfaces*, 2019, **6**, 1–27.
66 A. M. Coclite, R. M. Howden, D. C. Borrelli, C. D. Petruczok, R. Yang, J. L. Yagüe, A. Ugur, N. Chen, S. Lee, W. J. Jo, A. Liu, X. Wang and K. K. Gleason, *Adv. Mater.*, 2013, **25**, 5392–5423.
67 K. K. Gleason, *Nat. Rev. Phys.*, 2020, **2**, 347–364.
68 D. Bilger, S. Z. Homayounfar and T. L. Andrew, *J. Mater. Chem. C*, 2019, **7**, 7159–7174.
69 T. K. Das and S. Prusty, *Polym.-Plast. Technol. Eng.*, 2012, **51**, 1487–1500.
70 Y. Tan and K. Ghandi, *Synth. Met.*, 2013, **175**, 183–191.
71 E. M. Genies, G. Bidan and A. F. Diaz, *J. Electroanal. Chem.*, 1983, **149**, 101–113.
72 T. Yamamoto, *J. Organomet. Chem.*, 2002, **653**, 195–199.
73 T. Yamamoto, *Macromol. Rapid Commun.*, 2002, **23**, 583–6006.
74 S. Sadki, P. Schottland, N. Brodie and G. Sabouraud, *Chem. Soc. Rev.*, 2000, **29**, 283–293.
75 T. L. Kelly and M. O. Wolf, *Chem. Soc. Rev.*, 2010, **39**, 1526–1535.
76 T. Iyoda, M. Kitano and T. Shimidzu, *J. Chem. Soc., Chem. Commun.*, 1991, 1618–1619.
77 Y. Yagci, F. Yilmaz, S. Kiralp and L. Toppare, *Macromol. Chem. Phys.*, 2005, **206**, 1178–1182.
78 Y. Yagci, S. Jockusch and N. J. Turro, *Macromolecules*, 2007, **40**, 4481–4485.
79 E. M. Genies, G. Bidan and A. F. Diaz, *J. Electroanal. Chem.*, 1983, **149**, 101–113.
80 X. Liu, V. Sharapov, Z. Zhang, F. Wiser, M. A. Awais and L. Yu, *J. Mater. Chem. C*, 2020, **8**, 7026–7033.
81 E. F. Woods, A. J. Berl and J. A. Kalow, *Angew. Chem., Int. Ed.*, 2020, **59**, 6062–6067.
82 D. Bhattacharyya, R. M. Howden, D. C. Borrelli and K. K. Gleason, *J. Polym. Sci., Part B: Polym. Phys.*, 2012, **50**, 1329–1351.
83 L. M. H. Groenewoud, A. E. Weinbeck, G. H. M. Engbers and J. Feijen, *Synth. Met.*, 2002, **126**, 143–149.
84 L. Martin, J. Esteve and S. Borrós, *Thin Solid Films*, 2004, **451–452**, 74–80.
85 C. Nastase, F. Nastase, A. Dumitru, M. Ionescu and I. Stamatin, *Composites, Part A*, 2005, **36**, 481–485.
86 X. Y. Zhao, M. Z. Wang and J. Xiao, *Eur. Polym. J.*, 2006, **42**, 2161–2167.
87 X. Y. Zhao, M. Zhu Wang, Z. Wang and B. Zhu Zhang, *Thin Solid Films*, 2008, **516**, 8272–8277.
88 P. Yang, J. Zhang and Y. Guo, *Appl. Surf. Sci.*, 2009, **255**, 6924–6929.
89 T. Barman and A. R. Pal, *Appl. Surf. Sci.*, 2012, **259**, 691–697.
90 M. Rajabi, A. R. Ghassami, M. Abbasi Firouzjah, S. I. Hosseini and B. Shokri, *Plasma Chem. Plasma Process.*, 2013, **33**, 817–826.
91 C. S. Park, D. H. Kim, B. J. Shin, D. Y. Kim, H. K. Lee and H. S. Tae, *Materials*, 2016, **9**, 1–11.

92 C. S. Park, E. Y. Jung, D. H. Kim, D. Y. Kim, H. K. Lee, B. J. Shin, D. H. Lee and H. S. Tae, *Materials*, 2017, **10**, 1272.
93 S. Kim, J. S. Oh, T. Hwang, H. W. Seo, D. C. Jeong, J. H. Lee, L. Wen, C. Song, J. G. Han and J. Do Nam, *Macromol. Res.*, 2019, 243–249.
94 M. N. Subramaniam, P. S. Goh, W. J. Lau, A. F. Ismail, M. Gürsoy and M. Karaman, *Appl. Surf. Sci.*, 2019, **484**, 740–750.
95 P. D. Dapkus, *Annu. Rev. Mater. Sci.*, 1982, **12**, 243–269.
96 M. Meyyappan, *J. Phys. D: Appl. Phys.*, 2009, **42**, 213001.
97 S. M. George, *Chem. Rev.*, 2010, **110**, 111–131.
98 S. J. Yu, K. Pak, M. J. Kwak, M. Joo, B. J. Kim, M. S. Oh, J. Baek, H. Park, G. Choi, D. H. Kim, J. Choi, Y. Choi, J. Shin, H. Moon, E. Lee and S. G. Im, *Adv. Eng. Mater.*, 2018, **20**(3), 1700622.
99 S. G. Im and K. K. Gleason, *Macromolecules*, 2007, **40**, 6552–6556.
100 S. Nejati and K. K. S. Lau, *Langmuir*, 2011, **27**, 15223–15229.
101 Y. Y. Smolin, M. Soroush and K. K. S. Lau, *Beilstein J. Nanotechnol.*, 2017, **8**, 1266–1276.
102 K. Baba, G. Bengasi, D. El Assad, P. Grysan, E. Lentzen, K. Heinze, G. Frache and N. D. Boscher, *Eur. J. Org. Chem.*, 2019, 2368–2375.
103 N. Cheng, L. Zhang, J. Joon Kim and T. L. Andrew, *J. Mater. Chem. C*, 2017, **5**, 5787–5796.
104 G. Kaur, R. Adhikari, P. Cass, M. Bown and P. Gunatillake, *RSC Adv.*, 2015, **5**, 37553–37567.
105 D. Kumar and R. C. Sharma, *Eur. Polym. J.*, 1998, **34**, 1053–1060.
106 G. Bengasi, K. Baba, G. Frache, J. Desport, P. Gratia, K. Heinze and N. D. Boscher, *Angew. Chem., Int. Ed.*, 2019, **58**, 2103–2108.
107 H. Goktas, X. Wang, N. D. Boscher, S. Torosian and K. K. Gleason, *J. Mater. Chem. C*, 2016, **4**, 3403–3414.
108 O. Schäfer, A. Greiner, J. Pommerehne, W. Guss, H. Vestweber, H. Y. Tak, H. Bässler, C. Schmidt, G. Lüssem, B. Schartel, V. Stümpflen, J. H. Wendorff, S. Spiegel, C. Möller and H. W. Spiess, *Synth. Met.*, 1996, **82**, 1–9.
109 K. M. Vaeth and K. F. Jensen, *Macromolecules*, 1998, **31**, 6789–6793.
110 K. M. Vaeth and K. F. Jensen, *Appl. Phys. Lett.*, 1997, **71**, 2091–2093.
111 K. Kim, M. Y. Jung, G. L. Zhong, J. Il Jin, T. Y. Kim and D. J. Ahn, *Synth. Met.*, 2004, **144**, 7–11.
112 T. Yamamoto and T. Aki Koizumi, *Polymer*, 2007, **48**, 5449–5472.
113 T. Yamamoto, *Bull. Chem. Soc. Jpn.*, 2010, **83**, 431–455.
114 D. Cardenas-Morcoso, E. Vey, M. Heiderscheid, G. Frache and N. D. Boscher, *J. Mater. Chem. C*, 2022, **10**, 2194–2204.
115 J. Xu and K. K. Gleason, *ACS Appl. Mater. Interfaces*, 2011, **3**, 2410–2416.
116 R. W. Johnson, A. Hultqvist and S. F. Bent, *Mater. Today*, 2014, **17**, 236–246.
117 T. Q. Nguyen, R. Y. Yee and B. J. Schwartz, *J. Photochem. Photobiol., A*, 2001, **144**, 21–30.
118 Mezrlow, An Automated Irrigation System Using Arduino Microcontroller, 2011, 1908, 2–6.
119 R. Borjas and D. A. Buttry, *Chem. Mater.*, 1991, **3**, 872–878.
120 W. J. M. J. S. R. Jayasundara and G. Schreckenbach, *J. Phys. Chem. C*, 2020, **124**, 17528–17537.
121 Y. Sui, Y. Deng, T. Du, Y. Shi and Y. Geng, *Mater. Chem. Front.*, 2019, **3**, 1932–1951.
122 M. Goel, C. D. Heinrich, G. Krauss and M. Thelakkat, *Macromol. Rapid Commun.*, 2019, **40**, 1–31.
123 Z. Li, C. C. Chueh and A. K. Y. Jen, *Prog. Polym. Sci.*, 2019, **99**, 101175.
124 H. Jia and T. Lei, *J. Mater. Chem. C*, 2019, **7**, 12809–12821.
125 S. Nejati, T. E. Minford, Y. Y. Smolin and K. K. S. Lau, *ACS Nano*, 2014, **8**, 5413–5422.
126 D. C. Borrelli, S. Lee and K. K. Gleason, *J. Mater. Chem. C*, 2014, **2**, 7223–7231.
127 S. Lee, D. C. Borrelli and K. K. Gleason, *Org. Electron.*, 2016, **33**, 253–262.
128 S. Lee, D. C. Borrelli, W. J. Jo, A. S. Reed and K. K. Gleason, *Adv. Mater. Interfaces*, 2018, **5**, 1–8.
129 S. Vaddiraju, K. Seneca and K. K. Gleason, *Adv. Funct. Mater.*, 2008, **18**, 1929–1938.
130 A. Castro-Carranza, J. C. Nolasco, S. Bley, M. Rückmann, F. Meierhofer, L. Mädler, T. Voss and J. Gutowski, *J. Polym. Sci., Part B: Polym. Phys.*, 2016, **54**, 1537–1544.
131 M. C. Barr, J. A. Rowehl, R. R. Lunt, J. Xu, A. Wang, C. M. Boyce, S. G. Im, V. Bulović and K. K. Gleason, *Adv. Mater.*, 2011, **23**, 3500–3505.
132 H. Park, R. M. Howden, M. C. Barr, V. Bulović, K. Gleason and J. Kong, *ACS Nano*, 2012, **6**, 6370–6377.
133 N. Lachman, H. Xu, Y. Zhou, M. Ghaffari, M. Lin, D. Bhattacharyya, A. Ugur, K. K. Gleason, Q. M. Zhang and B. L. Wardle, *Adv. Mater. Interfaces*, 2014, **1**, 1–6.
134 X. Wang, A. Ugur, H. Goktas, N. Chen, M. Wang, N. Lachman, E. Kalfon-Cohen, W. Fang, B. L. Wardle and K. K. Gleason, *ACS Sens.*, 2016, **1**, 374–383.
135 S. Bley, M. Rückmann, A. Castro-Carranza, F. Meierhofer, L. Mädler, T. Voss and J. Gutowski, *Phys. Status Solidi C*, 2016, **13**, 614–617.
136 R. M. Howden, E. D. McVay and K. K. Gleason, *J. Mater. Chem. A*, 2013, **1**, 1334–1340.
137 J. P. Lock, J. L. Lutkenhaus, N. S. Zacharia, S. G. Im, P. T. Hammond and K. K. Gleason, *Synth. Met.*, 2007, **157**, 894–898.
138 A. Liu, P. Kovacik, N. Peard, W. Tian, H. Goktas, J. Lau, B. Dunn and K. K. Gleason, *Adv. Mater.*, 2017, **29**, 1606091.
139 E. F. G. Meysam Heydari Gharahcheshmeh, M. T. Robinson and K. K. Gleason, *Adv. Funct. Mater.*, 2021, **31**, 2008712.
140 X. Wang, X. Zhang, L. Sun, D. Lee, S. Lee, M. Wang, J. Zhao, Y. Shao-Horn, M. Dinca, T. Palacios and K. K. Gleason, *Sci. Adv.*, 2018, **4**, 5780.
141 D. Bhattacharyya and K. K. Gleason, *J. Mater. Chem.*, 2012, **22**, 405–410.
142 W. J. Jo, D. C. Borrelli, V. Bulović and K. K. Gleason, *Org. Electron.*, 2015, **26**, 55–60.

143 W. J. Jo, J. T. Nelson, S. Chang, V. Bulović, S. Gradečak, M. S. Strano and K. K. Gleason, *Adv. Mater.*, 2016, **28**, 6399–6404.
144 S. Vaddiraju and K. K. Gleason, *Nanotechnology*, 2010, **21**, 125503.
145 X. Wang, S. Hou, H. Goktas, P. Kovacik, F. Yaul, A. Paidimarri, N. Ickes, A. Chandrakasan and K. Gleason, *ACS Appl. Mater. Interfaces*, 2015, **7**, 16213–16222.
146 D. Bhattacharyya, K. Senecal, P. Marek, A. Senecal and K. K. Gleason, *Adv. Funct. Mater.*, 2011, **21**, 4328–4337.
147 D. C. Borrelli and K. K. Gleason, *Macromolecules*, 2013, **46**, 6169–6176.
148 S. Lee and K. K. Gleason, *Adv. Funct. Mater.*, 2015, **25**, 85–93.
149 T. L. Andrew, L. Zhang, N. Cheng, M. Baima, J. J. Kim, L. Allison and S. Hoxie, *Acc. Chem. Res.*, 2018, **51**, 850–859.
150 H. Coskun, A. Aljabour, P. De Luna, D. Farka, T. Greunz, D. Stifter, M. Kus, X. Zheng, M. Liu, A. W. Hassel, W. Schöfberger, E. H. Sargent, N. S. Sariciftci and P. Stadler, *Sci. Adv.*, 2017, **3**, 1–9.
151 H. Coskun, A. Aljabour, L. Uiberlacker, M. Strobel, S. Hild, C. Cobet, D. Farka, P. Stadler and N. S. Sariciftci, *Thin Solid Films*, 2018, **645**, 320–325.
152 Y. Xu, X. Wang, J. Zhou, B. Song, Z. Jiang, E. M. Y. Lee, S. Huberman, K. K. Gleason and G. Chen, *Sci. Adv.*, 2018, **4**, 3031.
153 M. Nojima, Y. Ohta and T. Yokozawa, *Kobunshi*, 2013, **62**, 236–238.
154 M. K. Jeong, E. H. Suh, K. Lee, J. Jang and I. H. Jung, *Org. Electron.*, 2020, **86**, 105921.
155 D. Qu, T. Qi and H. Huang, *J. Energy Chem.*, 2021, **59**, 364–387.
156 E. F. Woods, A. J. Berl and J. A. Kalow, *Angew. Chem.*, 2020, **132**, 6118–6123.
157 D. Bilger, K. W. Park and T. L. Andrew, *Synth. Met.*, 2019, **250**, 1–6.
158 H. Kuzmany and J. Kürti, *Synth. Met.*, 1987, **21**, 95–102.
159 J. L. Brédas, R. Silbey, D. S. Boudreaux and R. R. Chance, *J. Am. Chem. Soc.*, 1983, **105**, 6555–6559.
160 J. Mei and Z. Bao, *Chem. Mater.*, 2014, **26**, 604–615.
161 K. Chung, A. McAllister, D. Bilby, B. G. Kim, M. S. Kwon, E. Kioupakis and J. Kim, *Chem. Sci.*, 2015, **6**, 6980–6985.
162 Z. Fan, D. Du, H. Yao and J. Ouyang, *ACS Appl. Mater. Interfaces*, 2017, **9**, 11732–11738.
163 S. Hayashi, S. I. Yamamoto and T. Koizumi, *Sci. Rep.*, 2017, **7**, 1–8.
164 J. S. Wu, Y. J. Cheng, M. Dubosc, C. H. Hsieh, C. Y. Chang and C. S. Hsu, *Chem. Commun.*, 2010, **46**, 3259–3261.
165 A. T. Lawal and G. G. Wallace, *Talanta*, 2014, **119**, 133–143.
166 R. Brooke, P. Cottis, P. Talemi, M. Fabretto, P. Murphy and D. Evans, *Prog. Mater. Sci.*, 2017, **86**, 127–146.
167 K. G. Neoh, E. T. Kang and K. L. Tan, *Polymer*, 1993, **34**, 3921–3928.
168 C. Kranz, M. Ludwig, H. E. Gaub and W. Schuhmann, *Adv. Mater.*, 1995, **7**, 38–40.
169 P. P. Sengupta, P. Kar and B. Adhikari, *Thin Solid Films*, 2009, **517**, 3770–3775.
170 F. Ghamouss, A. Brugère, A. C. Anbalagan, B. Schmaltz, E. Luais and F. Tran-Van, *Synth. Met.*, 2013, **168**, 9–15.
171 N. Y. Abu-Thabit, *J. Chem. Educ.*, 2016, **93**, 1606–1611.
172 D. L. Meyer, N. Schmidt-Meinzer, C. Matt, S. Rein, F. Lombeck, M. Sommer and T. Biskup, *J. Phys. Chem. C*, 2019, **123**, 20071–20083.
173 L. Zhu, C. Jiang, G. Chen, Z. Zhou and Q. Li, *Org. Electron.*, 2017, **49**, 278–285.
174 Y. Y. Smolin, K. L. Van Aken, M. Boota, M. Soroush, Y. Gogotsi and K. K. S. Lau, *Adv. Mater. Interfaces*, 2017, **4**, 1601201.
175 J. Stejskal and M. Trchová, *Polym. Int.*, 2012, **61**, 240–251.
176 H. Chelawat, S. Vaddiraju and K. Gleason, *Chem. Mater.*, 2010, **22**, 2864–2868.
177 R. D. McCullough, R. D. Lowe, M. Jayaraman and D. L. Anderson, *J. Org. Chem.*, 1993, **58**, 904–912.
178 T. A. Chen, X. Wu and R. D. Rieke, *J. Am. Chem. Soc.*, 1995, **117**, 233–244.
179 R. D. Mccullough and R. D. Lowe, *J. Chem. Soc., Chem. Commun.*, 1992, 70–72.
180 R. D. McCullough, P. C. Ewbank and R. S. Loewe, *J. Am. Chem. Soc.*, 1997, **119**, 633–634.
181 R. D. McCullough, S. P. Williams, R. D. Lowe, M. Jayaraman and S. Tristram-Nagle, *J. Am. Chem. Soc.*, 1993, **115**, 4910–4911.
182 T. A. Chen and R. D. Rieke, *J. Am. Chem. Soc.*, 1992, **114**, 10087–10088.
183 M. R. Andersson, D. Seise, M. Berggren, H. Järvinen, I. T. Hjertberg, O. Inganás, O. Wennerstrom and J. Österholm, *Macromolecules*, 1994, **27**, 6503–6506.
184 X. Shen, W. Hu and T. P. Russell, *Macromolecules*, 2016, **49**, 4501–4509.
185 D. Alberga, A. Perrier, I. Ciofini, G. F. Mangiatordi, G. Lattanzi and C. Adamo, *Phys. Chem. Chem. Phys.*, 2015, **17**, 18742–18750.
186 X. Wang, X. Zhang, L. Sun, D. Lee, S. Lee, M. Wang, J. Zhao, Y. Shao-Horn, M. Dinca, T. Palacios and K. K. Gleason, *Sci. Adv.*, 2018, **4**, 1–10.
187 R. Noriega, J. Rivnay, K. Vandewal, F. P. V. Koch, N. Stingelin, P. Smith, M. F. Toney and A. Salleo, *Nat. Mater.*, 2013, **12**, 1038–1044.
188 D. T. Scholes, P. Y. Yee, J. R. Lindemuth, H. Kang, J. Onorato, R. Ghosh, C. K. Luscombe, F. C. Spano, S. H. Tolbert and B. J. Schwartz, *Adv. Funct. Mater.*, 2017, **27**, 1702654.
189 K. Ueji, M. Ohno, J. Takeya and S. Watanabe, *Appl. Phys. Express*, 2018, **12**, 011004.
190 D. T. Scholes, P. Y. Yee, G. R. McKeown, S. Li, H. Kang, J. R. Lindemuth, X. Xia, S. C. King, D. S. Seferos, S. H. Tolbert and B. J. Schwartz, *Chem. Mater.*, 2019, **31**, 73–82.
191 H. Y. Park, H. Yang, S. K. Choi and S. Y. Jang, *ACS Appl. Mater. Interfaces*, 2012, **4**, 214–221.
192 K. Lee, M. K. Jeong, E. H. Suh, W. J. Jeong, J. G. Oh, J. Jang and I. H. Jung, *Adv. Electron. Mater.*, 2022, **8**, 1–11.
193 F. Zhang, E. Mohammadi, X. Luo, J. Strzalka, J. Mei and Y. Diao, *Langmuir*, 2018, **34**, 1109–1122.

194 A. Zen, M. Saphiannikova, D. Neher, J. Grenzer, S. Grigorian, U. Pietsch, U. Asawapirom, S. Janietz, U. Scherf, I. Lieberwirth and G. Wegner, *Macromolecules*, 2006, **39**, 2162–2171.
195 M. A. Ruderer, S. Guo, R. Meier, H. Y. Chiang, V. Körstgens, J. Wiedersich, J. Perlich, S. V. Roth and P. Müller-Buschbaum, *Adv. Funct. Mater.*, 2011, **21**, 3382–3391.
196 J. Liu, Y. Sun, X. Gao, R. Xing, L. Zheng, S. Wu, Y. Geng and Y. Han, *Langmuir*, 2011, **27**, 4212–4219.
197 M. H. Rezvani, F. Farajollahi, A. Nikfarjam, P. Bakhtiarpour and E. Saydanzad, *Materials*, 2013, **6**, 1994–2006.
198 D. Alberga, G. F. Mangiatordi, L. Torsi and G. Lattanzi, *J. Phys. Chem. C*, 2014, **118**, 8641–8655.
199 S. Sanda, R. Nakamichi, T. Nagase, T. Kobayashi, K. Takimiya, Y. Sadamitsu and H. Naito, *Org. Electron.*, 2019, **69**, 181–189.
200 T. J. M. Choongik Kim and A. Facchetti, *Science*, 2007, **318**, 76–80.
201 E. Mohammadi, G. Qu, P. Kafle, S. H. Jung, J. K. Lee and Y. Diao, *Mol. Syst. Des. Eng.*, 2020, **5**, 125–138.
202 G. Jo, J. Jung and M. Chang, *Polymers*, 2019, **11**, 332.
203 J. S. Kim, Y. Park, D. Y. Lee, J. H. Lee, J. H. Park, J. K. Kim and K. Cho, *Adv. Funct. Mater.*, 2010, **20**, 540–545.
204 P. L. Danielsen, *J. Phys. C: Solid State Phys.*, 1986, **19**, L741.
205 Y. Yao, H. Dong and W. Hu, *Polym. Chem.*, 2013, **4**, 5197–5205.
206 K. S. Ahn, H. Jo, J. B. Kim, I. Seo, H. H. Lee and D. R. Lee, *ACS Appl. Mater. Interfaces*, 2020, **12**, 1142–1150.
207 X. Wang, W. Deng, Y. Chen, X. Wang, P. Ye, X. Wu, C. Yan, X. Zhan, F. Liu and H. Huang, *J. Mater. Chem. A*, 2017, **5**, 5585–5593.
208 M. S. Chen, J. R. Niskala, D. A. Unruh, C. K. Chu, O. P. Lee and J. M. J. Fréchet, *Chem. Mater.*, 2013, **25**, 4088–4096.
209 M. S. Chen, J. R. Niskala, D. A. Unruh, C. K. Chu, O. P. Lee and J. M. J. Fréchet, *Chem. Mater.*, 2013, **25**, 4088–4096.
210 R. Rieger, D. Beckmann, A. Mavrinskiy, M. Kastler and K. Müllen, *Chem. Mater.*, 2010, **22**, 5314–5318.
211 M. Pandey, N. Kumari, S. Nagamatsu and S. S. Pandey, *J. Mater. Chem. C*, 2019, **7**, 13323–13351.
212 G. Giri, D. M. Delongchamp, J. Reinspach, D. A. Fischer, L. J. Richter, J. Xu, S. Benight, A. Ayzner, M. He, L. Fang, G. Xue, M. F. Toney and Z. Bao, *Chem. Mater.*, 2015, **27**, 2350–2359.
213 M. Brinkmann, L. Hartmann, L. Biniek, K. Tremel and N. Kayunkid, *Macromol. Rapid Commun.*, 2014, **35**, 9–26.
214 M. H. Gharahcheshmeh, M. M. Tavakoli, E. F. Gleason, M. T. Robinson, J. Kong and K. K. Gleason, *Sci. Adv.*, 2019, **5**, 1–13.
215 W. Ma, K. Shi, Y. Wu, Z. Y. Lu, H. Y. Liu, J. Y. Wang and J. Pei, *ACS Appl. Mater. Interfaces*, 2016, **8**, 24737–24743.
216 C. M. Palumbiny, F. Liu, T. P. Russell, A. Hexemer, C. Wang and P. Müller-Buschbaum, *Adv. Mater.*, 2015, **27**, 3391–3397.
217 I. Petsagkourakis, E. Pavlopoulou, G. Portale, B. A. Kuropatwa, S. Dilhaire, G. Fleury and G. Hadziioannou, *Sci. Rep.*, 2016, **6**, 1–8.
218 S. Kee, N. Kim, B. S. Kim, S. Park, Y. H. Jang, S. H. Lee, J. Kim, J. Kim, S. Kwon and K. Lee, *Adv. Mater.*, 2016, **28**, 8625–8631.
219 T. Lee, W. Kwon and M. Park, *Org. Electron.*, 2019, **67**, 26–33.
220 M. N. Gueye, A. Carella, N. Massonnet, E. Yvenou, S. Brenet, J. Faure-Vincent, S. Pouget, F. Rieutord, H. Okuno, A. Benayad, R. Demadrille and J. P. Simonato, *Chem. Mater.*, 2016, **28**, 3462–3468.
221 D. Bhattacharyya and K. K. Gleason, *Chem. Mater.*, 2011, **23**, 2600–2605.
222 S. G. Im, D. Kusters, W. Choi, S. H. Baxamusa, M. C. M. van de Sanden and K. K. Gleason, *ACS Nano*, 2008, **2**, 1959–1967.
223 S. Kaviani, M. Mohammadi Ghaleni, E. Tavakoli and S. Nejati, *ACS Appl. Polym. Mater.*, 2019, **1**, 552–560.
224 Y. Y. Smolin, M. Soroush and K. K. S. Lau, *Ind. Eng. Chem. Res.*, 2017, **56**, 6221–6228.
225 S. E. Atanasov, M. D. Losego, B. Gong, E. Sachet, J. P. Maria, P. S. Williams and G. N. Parsons, *Chem. Mater.*, 2014, **26**, 3471–3478.
226 R. G. Larson, *Nature*, 2017, **550**, 466–467.
227 J. Chang, Z. Lin, J. Li, S. L. Lim, F. Wang, G. Li, J. Zhang and J. Wu, *Adv. Electron. Mater.*, 2015, **1**, 1–9.
228 A. Teichler, J. Perelaer and U. S. Schubert, *J. Mater. Chem. C*, 2013, **1**, 1910–1925.
229 C. S. Lee, W. Yin, A. P. Holt, J. R. Sangoro, A. P. Sokolov and M. D. Dadmun, *Adv. Funct. Mater.*, 2015, **25**, 5848–5857.
230 K. B. Burke, W. J. Belcher, L. Thomsen, B. Watts, C. R. McNeill, H. Ade and P. C. Dastoor, *Macromolecules*, 2009, **42**, 3098–3103.
231 R. Meier, M. Schindler, P. Müller-Buschbaum and B. Watts, *Phys. Rev. B: Condens. Matter Mater. Phys.*, 2011, **84**, 1–6.
232 P. Moni, A. Al-Obeidi and K. K. Gleason, *Beilstein J. Nanotechnol.*, 2017, **8**, 723–735.
233 K. K. Gleason, *CVD Polymers: Fabrication of Organic Surfaces and Devices*, 2015, 1, pp.1–11.
234 D. E. Weidner, L. W. Schwartz and R. R. Eley, *J. Colloid Interface Sci.*, 1996, **179**, 66–75.
235 F. Zhang, G. Baralia, A. Boborodea, C. Bailly, B. Nysten and A. M. Jonas, *Langmuir*, 2005, **21**, 7427–7432.
236 L. E. Stillwagon and R. G. Larson, *Phys. Fluids A*, 1992, **4**, 895–903.
237 A. Dianatdar, PhD thesis, University of Groningen, 2022.
238 K. L. Mittal, *Polym. Eng. Sci.*, 1977, **17**, 467–473.
239 J. O. Carneiro, V. Teixeira and S. Azevedo, *Encyclopedia of Thermal Stresses*, 2014, pp.4222–4231.
240 X. Wang, K. Chen, L. S. de Vasconcelos, J. He, Y. C. Shin, J. Mei and K. Zhao, *Nat. Commun.*, 2020, **11**, 1–10.
241 M. Lane, *Annu. Rev. Mater. Res.*, 2003, **33**, 29–54.
242 G. Yan and J. R. White, *Polym. Eng. Sci.*, 1999, **39**, 1856–1865.
243 R. Katsumata, S. Ata, K. Kuboyama and T. Ougizawa, *J. Appl. Polym. Sci.*, 2013, **128**, 60–65.
244 J. Y. Chung, T. Q. Chastek, M. J. Fasolka, H. W. Ro and C. M. Stafford, *ACS Nano*, 2009, **3**, 844–852.

245 H. Zhang and L. Zhang, *Appl. Phys. Lett.*, 2016, **106**, 033102.
246 P. T. Chen, Y. W. Yang, G. Reiter and A. C. M. Yang, *Polymer*, 2020, **204**, 122753.
247 S. G. Croll, *J. Appl. Polym. Sci.*, 1979, **23**, 847–858.
248 M. Ree, C. W. Chu and M. J. Goldberg, *J. Appl. Phys.*, 1994, **75**, 1410–1419.
249 G. Abadias, E. Chason, J. Keckes, M. Sebastiani, G. B. Thompson, E. Barthel, G. L. Doll, C. E. Murray, C. H. Stoessel and L. Martinu, *J. Vac. Sci. Technol., A*, 2018, **36**, 020801.
250 L. Ouyang, B. Wei, C. Chen Kuo, S. Pathak, B. Farrell and D. C. Martin, *Sci. Adv.*, 2017, **3**, 1–12.
251 B. Wei, J. Liu, L. Ouyang, C. C. Kuo and D. C. Martin, *ACS Appl. Mater. Interfaces*, 2015, **7**, 15388–15394.
252 S. K. Sontag, N. Marshall and J. Locklin, *Chem. Commun.*, 2009, 3354–3356.
253 B. Yameen, C. Rodriguez-Emmenegger, C. M. Preuss, O. Pop-Georgievski, E. Verveniotis, V. Trouillet, B. Rezek and C. Barner-Kowollik, *Chem. Commun.*, 2013, **49**, 8623–8625.
254 P. Kovacic and M. B. Jones, *Chem. Rev.*, 1987, **87**, 357–379.
255 S. G. Im, P. J. Yoo, P. T. Hammond and K. K. Gleason, *Adv. Mater.*, 2007, **19**, 2863–2867.
256 A. J. Clancy, M. K. Bayazit, S. A. Hodge, N. T. Skipper, C. A. Howard and M. S. P. Shaffer, *Chem. Rev.*, 2018, **118**, 7363–7408.
257 S. Byun, J. Choi, Y. Roh, D. Song, M. H. Ryou and Y. M. Lee, *Electrochim. Acta*, 2020, **332**, 135471.
258 M. A. del Valle, M. A. Gacitúa, F. Hernández, M. Luengo and L. A. Hernández, *Polymers*, 2023, **15**, 1450.
259 D. H. Kim, S. E. Atanasov, P. Lemaire, K. Lee and G. N. Parsons, *ACS Appl. Mater. Interfaces*, 2015, **7**, 3866–3870.
260 R. M. Howden, E. J. Flores, V. Bulović and K. K. Gleason, *Org. Electron.*, 2013, **14**, 2257–2268.
261 A. M. Gaikwad, Y. Khan, A. E. Ostfeld, S. Pandya, S. Abraham and A. C. Arias, *Org. Electron.*, 2016, **30**, 18–29.
262 E. Singh, M. Meyyappan and H. S. Nalwa, *ACS Appl. Mater. Interfaces*, 2017, **9**, 34544–34586.
263 R. Fan and T. L. Andrew, *J. Electrochem. Soc.*, 2020, **167**, 037542.
264 L. Zhang and T. L. Andrew, *ACS Appl. Mater. Interfaces*, 2018, **10**, 38574–38580.
265 L. Zhang, W. Viola and T. L. Andrew, *ACS Appl. Mater. Interfaces*, 2018, **10**, 36834–36840.
266 W. Viola, C. Jin and T. L. Andrew, *Synth. Met.*, 2020, **268**, 116483.
267 L. K. Allison, S. Rostaminia, A. Kiaghadi, D. Ganesan and T. L. Andrew, *ACS Omega*, 2021, **6**, 31869–31875.
268 J. J. Kim, L. K. Allison and T. L. Andrew, *Sci. Adv.*, 2019, **5**, 0463.
269 A. Castro-Carranza, J. C. Nolasco, S. Bley, M. Rückmann, F. Meierhofer, L. Mädler, T. Voss and J. Gutowski, *J. Polym. Sci., Part B: Polym. Phys.*, 2016, **54**, 1537–1544.
270 L.-C. Chao and E.-P. Chang, *J. Appl. Polym. Sci.*, 1981, **26**, 603–610.
271 D. C. Dragunski, A. R. Freitas, A. F. Rubira and E. C. Muniz, *Polym. Degrad. Stab.*, 2000, **67**, 239–247.
272 P. Kovacik, G. del Hierro, W. Livernois and K. K. Gleason, *Mater. Horiz.*, 2015, **2**, 221–227.
273 H. K. H. Lee, Z. Li, I. Constantinou, F. So, S. W. Tsang and S. K. So, *Adv. Energy Mater.*, 2014, **4**, 1400768.
274 L. Mockus, J. J. Peterson, J. M. Lainez and G. V. Reklaitis, *Org. Process Res. Dev.*, 2015, **19**, 908–914.
275 W. Shin, W. Ko, S. H. Jin, T. Earmme and Y. J. Hwang, *Chem. Eng. J.*, 2021, **412**, 128572.
276 M. P. Aplan and E. D. Gomez, *Ind. Eng. Chem. Res.*, 2017, **56**, 7888–7901.
277 H. Seyler, D. J. Jones, A. B. Holmes and W. W. H. Wong, *Chem. Commun.*, 2012, **48**, 1598–1600.
278 P. Serp, P. Kalck and R. Feurer, *Chem. Rev.*, 2002, **102**, 3085–3128.
279 M. Mirabedin, H. Vergnes, N. Caussé, C. Vahlas and B. Caussat, *Appl. Surf. Sci.*, 2021, **554**, 149501.
280 G. Drewelow, H. Wook Song, Z. T. Jiang and S. Lee, *Appl. Surf. Sci.*, 2020, **501**, 144105.
281 S. H. Baxamusa, S. G. Im and K. K. Gleason, *Phys. Chem. Chem. Phys.*, 2009, **11**, 5227–5240.
282 K.-H. Dahmen, in*Encyclopedia of Physical Science and Technology*, ed. R. A. Meyers, Academic Press, San Diego, 3rd edn, 2002, vol. 2, pp.787–808.

